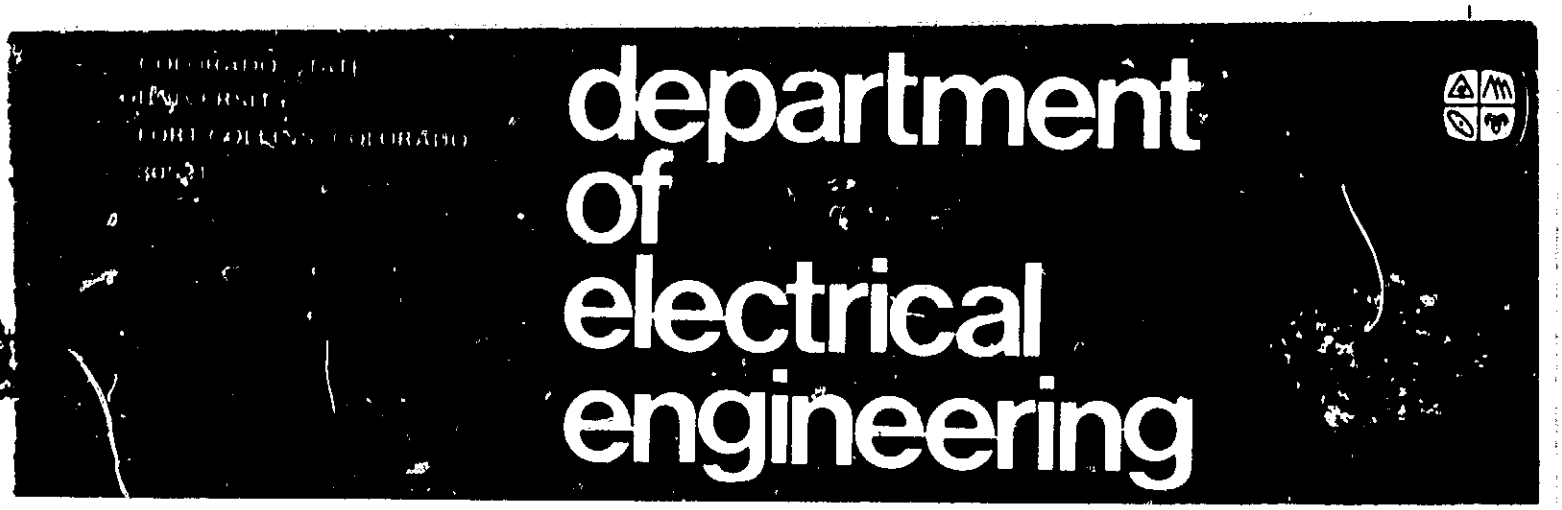

ANNUAL REPORT

THEORETICAL INVESTIGATIONS ON PLASMA PROCESSES IN THE KAUFMAN THRUSTER

by

H. E. Wilhelm

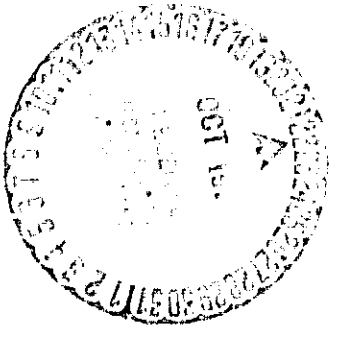

Prepared for

LEWIS RESEARCH CENTER

NATIONAL AERONAUTICS AND SPACE ADMINISTRATION

Grant NGR-06-002-147

September 1974

ANNUAL REPORT

THEORETICAL INVESTIGATIONS ON PLASMA PROCESSES IN THE KAUFMAN THRUSTER

by

H. E. Wilhelm

Prepared for

LEWIS RESEARCH CENTER

NATIONAL AERONAUTICS AND SPACE ADMINISTRATION

Grant NGR-06-002-147

September 1974

Department of Electrical Engineering

Colorado State University

Fort Collins, Colorado

FOREWORD

The theoretical work on plasma processes in the Kaufman ion propulsion system contained in this report has been supported by the NATIONAL AERONAUTICS AND SPACE ADMINISTRATION under Grant NGR - 06 - 002 - 147. This research has been monitored by Dr. John Serafini, NASA LEWIS RESEARCH CENTER.

CONTENTS

0. INTRODUCTION

The Grant NGR-06-002-147, "Theoretical Investigations on Plasma Processes in the Kaufman Thruster," is concerned with I) the sputtering of the accelerating grid, II) the sputtering of the cathodes of the hollow cathode and neutralizer discharges, III) the deposition of the sputtered atoms on system components such as the solar energy collectors, and the IV) hollow cathode and neutralizer discharge characteristics. The progress made on these subjects in the period from 6.1.73 to 6.15.74 is communicated herein.

In Part I, an analysis of the sputtering of metal surfaces and grids by ions of medium energies ($\varepsilon \sim 10^3$ eV) is given. The sputtering is explained by discontinuous, nonlinear thermal waves (generated by the impinging ion) which produce a spatially concentrated emission of metal atoms under strong nonequilibrium conditions. It is shown that the conventional parabolic (approximation) heat conduction equation can not describe the transient transport of heat in metals at high temperatures ($t \gtrsim 300°K$) and has to be replaced by an exact, nonlinear, hyperbolic wave equation for the temperature field. This approach leads to a theoretical prediction of the threshold energy for sputtering and to a quantitative theory of the sputtering rate. As concrete applications, i) the number of atoms sputtered from the accelerating grid by a charge exchange ion beam and ii) the sputtering of system components by micrometeorites are discussed briefly.

In Part II, a quantum statistical and a perturbation theoretical analysis of surface sputtering by ions of low energy ($\varepsilon < 10^2$ eV) is presented. Both approaches lead essentially to the same expression for

sputtering rate, i.e. dependence on the ion energy, atom density of the solid, the atom and ion masses, and scattering cross section. The theoretical sputtering rate formula agrees well with experimental data, in particular as to the threshold energy and the energy dependence. As an application, the number of atoms sputtered from the cathode of low pressure discharges is calculated. The underlying model assumes that a quasi-thermal ion beam is formed in the potential drop of the cathode sheath.

In Part III, the deposition of sputtered atoms on system components is treated. The transport model assumes that the sputtered atoms do not interact with themselves or any of the plasma particles (transport by free atomic flow). Analytical formulae for the deposition rate are given in the case of uniform, nonuniform parabolic, and arbitrary nonuniform emission sources. Only such system surfaces are considered which can be seen along straight lines from the emitter.

In Part IV, the theoretical efforts in determining the potential distribution and the particle velocity distributions in low pressure discharges, such as the hollow cathode and neutralizer discharges, are briefly discussed. Although two additional months were invested in the resolution of these problems, it was not possible to complete it because of mathematical difficulties. It is shown that the description of a collisionless electrical discharge leads to a nonlinear boundary-value problem for the coupled Vlasov equations

and the Poisson equation for the electron and ion components, which has functional boundary conditions. In spite of a significant effort, it was not possible to determine the specific discontinuous functional solutions which satisfy the nonlinear functional boundary-value problem. The purpose of the investigation is to calculate the potential distribution, in particular the cathode and anode falls, and the electron and ion velocity distributions. The velocity distribution of the ions is of interest in connection with the sputtering at the cathode. It is hoped that this investigation can be completed at a later date.

The investigations reported herein represent preliminary communications. An extended version of this work will be communicated in form of publications. In the past research period, the following investigations were published:

1. H. E. Wilhelm, Transient Ion Neutralization by Electrons, J. Appl. Phys. 44, 4562 (1973).

2. H. E. Wilhelm, Intercomponent Momentum Transport and Electrical Conductivity of Collisionless Plasma, Can. J. Phys. 51, 2468 (1973).

3. H. E. Wilhelm, Nonlinear Theory of Electron Neutralization Waves in Ion Beams with Dissipation, Phys. Fluids 17 (1974).

I. CONTRIBUTIONS TO VOLUME SPUTTERING

1. PROBLEM AND FOUNDATIONS

In the evaluation of the sputtering of metal surfaces (cathodes, grids), two classical problems are encountered, i) the determination of the energy distribution of the sputtering ions at the metal surface (kinetic problem) and ii) the calculation of the number of atoms ejected by an ion of given energy based on a physical model for the sputtering mechanism. The phenomenological approach to the sputtering process by von Hippel-Townes[1-2] assumes a Gaussian temperature distribution $T(r,t)$ around the point of impact of the ion at the metal surface which reaches to infinity (infinite speed of heat propagation) and flattens out as time increases, $T(r,t) \to 0$ for $t \to \infty$. The vapor pressure $P(r,t)$ of the metal is assumed[1-2] to adjust itself instantaneously to this transient temperature distribution in accordance with statistical equilibrium mechanics,

$$P(T) = (18\pi M\omega_D^2)^{3/2}/kT)^{-1/2} \exp(-E_s/kT)$$

where E_s is the sublimation energy and $\omega_D = k\theta_D/2\hbar$ a frequency related to the Debye-temperature θ_D[3]. This approach is unrealistic in the treatment or the thermal dissipation of the ion energy and assumes a physically unrealizable transient metal vapor equilibrium. As one sees from the above formula, the von Hippel-Townes model does not give a threshold energy for sputtering (since $P > 0$ for any $T > 0$) as observed in experiments.[4-5]

The other theoretical approaches are based on considerations of momentum conservation ("focusing collision sequences").[6-8] They

predict a threshold energy for sputtering which depends strongly on the masses of the ion and the metal atom.[6-8] This result is in direct disagreement with the experimentally determined threshold energies which are of the order of the dislocation energy of an atom in the metal lattice.[4-5]

The theoretical models used in these attempts[1-2,6-8] at explaining the sputtering process contain phenomenological parameters. Their success in explaining experimental observations appears to be due mainly to a proper adjustment of the phenomenological constants in each case. In the following, we try to develop a volume sputtering theory ($\varepsilon > 10^2$eV) which is free from phenomenological parameters. We show that the impinging ion, which penetrates through a certain number of atomic layers in the metal, generates a non-linear, discontinuous thermal wave. As a result of the high concentration of energy behind the wave front, the thermal wave produces a mechanism which breaks the atoms out of their bound places in the lattice. The metal atoms in the volume overrun by the thermal wave are emitted until the energy behind the wave front has decreased down to the dislocation energy of an atom. This concept leads directly to the correct threshold energy for sputtering. A theory of surface sputtering ($\varepsilon < 10^2$eV) is presented in Section II.

In the slowing down process of an ion penetrating into a metal, its kinetic energy ε is dissipated nearly homogeneously along its path of length L.[9] Accordingly, the energy expended per unit path length is in this approximation

$$\bar{\varepsilon} = \varepsilon/L \ [\text{erg cm}^{-1}]$$

where ε is the known ion energy, while L can be calculated from slowing down theory for charged particles in solids.[9] The energy ε of the ion appears quasi-instantaneously in form of thermal energy due to the high density of the metal (relaxation time $\sim 10^{-19}$ sec). Thus, a cylindrical thermal wave is generated by the ion with the path L as symmetry axis. (In case of low ion energies, when only one or a few atomic layers are penetrated by the ion, an essentially semi-spherical thermal wave is generated around the point of impact.)

The transport of heat in a metal is described by the relaxation equation for the heat flux $\vec{q}$ and the conservation equation for the thermal energy density ρcT (ρ = mass density, c = specific heat, T = absolute temperature). These equations are derived as moments of the Boltzmann equation, and are:

$$\frac{\partial \vec{q}}{\partial t} = -\frac{1}{\tau}\vec{q} - \frac{\lambda}{\tau}\nabla T \quad , \qquad (1)$$

$$\rho c \frac{\partial T}{\partial t} = -\nabla . \vec{q} \quad , \qquad (2)$$

where

$$\tau = \tau(T) \equiv \tau_o T^m, \qquad [\tau_o] = \text{sec deg}^{-m} \quad , \qquad (3)$$

$$\lambda = \lambda(T) \equiv \lambda_o T^n, \ [\lambda_o] = \text{erg cm}^{-1}\text{sec}^{-1}\text{deg}^{-n-1} \quad , \qquad (4)$$

are the relaxation time of the heat flux and the thermal conductivity of the metal, respectively. The temperature dependence of τ and λ can be modelled in wide temperature ranges by simple power relations ($m, n \gtrless 0$). Theory and measurements indicate that $\lambda \sim T^{+1}$ at low temperatures,

$\lambda \sim T^{-2}$ at intermediate temperatures, and $\lambda \sim T^{0}$ at high temperatures.[10] Since the electrical conductivity of the metal, $\sigma = (n_e e^2/m_e)\tau^*$, is proportional to the momentum relaxation time, τ is given in terms of λ by the Wiedemann-Franz relation[10]

$$\tau(T) = \frac{3}{\pi^3}\frac{m_e}{k^2}\frac{\lambda(T)}{n_e T} \tag{5}$$

where the electron density n_e is to be considered a constant ($\rho c = \rho_o c_o$ for a quasi-incompressible metal). Consideration will be given exclusively to cylindrical thermal waves.

2. PARABOLIC THERMAL WAVES

In contemporary heat transport theory,[11] it is standard to assume that a temperature gradient ∇T produces instantaneously a heat flux $\vec{q}$, i.e. Eq. (1) is replaced by $q = -\lambda \nabla T$. Combining this relation with Eq. (2) gives the usual parabolic heat conduction equation.[11] The initial-value problem for cylindrical thermal waves becomes in this approximation:

$$\frac{\partial T}{\partial t} = a \frac{1}{r} \frac{\partial}{\partial r} \left(T^n \frac{\partial T}{\partial r} \right) \tag{6}$$

where

$$2\pi \int_0^\infty T(r,t)\, r dr = Q \tag{7}$$

expresses the conservation of energy deposited per unit length by the ion, and

$$a \equiv \lambda_o / \rho c \qquad [\mathrm{cm}^2\ \mathrm{sec}^{-1}\ \mathrm{deg}^{-n}] \quad , \tag{8}$$

$$Q \equiv \bar{\varepsilon} / \rho c \qquad [\mathrm{deg}\ \mathrm{cm}^2] \quad . \tag{9}$$

Eq. (7) is mathematically equivalent to the initial condition, $T(r, t = 0) = Q\, \delta(r)/2\pi r$. The parameters a, Q and x, t permit the formation of a single nondimensional combination,

$$\xi = r / (a Q^n t)^{\frac{1}{2(n+1)}} \quad . \tag{10}$$

which has the meaning of the similarity variable of Eqs. (6) - (7). For dimensional reasons, one makes for the temperature field the ansatz

$$T = (Q/at)^{\frac{1}{n+1}} f(\xi) \quad . \tag{11}$$

Eq. (11) reduces Eqs. (6) - (7) to an ordinary nonlinear problem for the nondimensional function $f(\xi)$,

$$2(n+1)\frac{d}{d\xi}\left(f^n\xi\frac{df}{d\xi}\right)+\xi^2\frac{df}{d\xi}+2\xi f=0 \quad , \qquad (12)$$

where

$$2\pi\int_0^\infty f(\xi)\,\xi\,d\xi=1 \quad . \qquad (13)$$

Eq. (13) has a closed form solution which is discontinuous [$H(x)=1$, $x\geq+0$; $H(x)=0$, $x\leq-0$]:

$$f(\xi)=\left[\frac{n}{4(n+1)}\left(\xi_o^2-\xi^2\right)\right]^{\frac{1}{n}}H(\xi_o-\xi) \qquad (14)$$

where

$$\xi_o^{-\frac{2(n+1)}{n}}=\pi\left[\frac{n}{4(n+1)}\right]^{\frac{1}{n}}\int_0^1(1-\eta)^{\frac{1}{n}}\,d\eta$$

i.e.

$$\xi_o^2=\left(4^{\frac{1}{n}}/\pi\right)^{\frac{n}{n+1}}\frac{n+1}{n} \qquad (15)$$

by Eq. (13). It is physically more illustrative to rewrite the temperature distribution of the thermal wave as

$$T(r,t)=\hat{T}(t)\left[1-\frac{r^2}{R^2(t)}\right]^{\frac{1}{n}}H[R(t)-r] \qquad (16)$$

where

$$\hat{T}(t)=\pi[n/4(n+1)]^{\frac{1}{n}}\,\xi_o^{2(n+1)/n}\,\bar{T}/t) \quad , \qquad (17)$$

$$\bar{T}(t)=Q/\pi R^2(t) \quad , \qquad (18)$$

and

$$R(t) = \xi_o (aQ^n t)^{\frac{1}{2(n+1)}} \quad . \qquad (19)$$

Eq. (16) indicates that the temperature in the wave drops discontinuously to zero at $r = R(t)$, the position of the wave front. A nearly homogeneous concentration of thermal energy exists behind the thermal wave front, $0 \leq r \leq R(t)$, which advances with the speed

$$\frac{dR(t)}{dt} = \frac{\xi_o}{2(n+1)} t^{-1} (aQ^n t)^{\frac{1}{2(n+1)}} \quad . \qquad (20)$$

It should be noted that the parabolic solution in Eq. (16) diverges for $n < 0$ at $r = R(t)$, and reduces to an unrealistic Gaussian distribution which extends to infinity at any time $0 < t < \infty$ in the linear case, $n = 0$. Accordingly, for media with λ decreasing with increasing T or constant $\lambda (n \leq 0)$, Eq. (16) does not represent a useful approximation. As will be shown, these difficulties are removable by means of Eq. (1) which takes into consideration the physically required relaxation in any transient heat flow.

The propagation of a parabolic thermal wave in barium oxyde (BaO) is shown in Fig. 1 ($n = 3$).

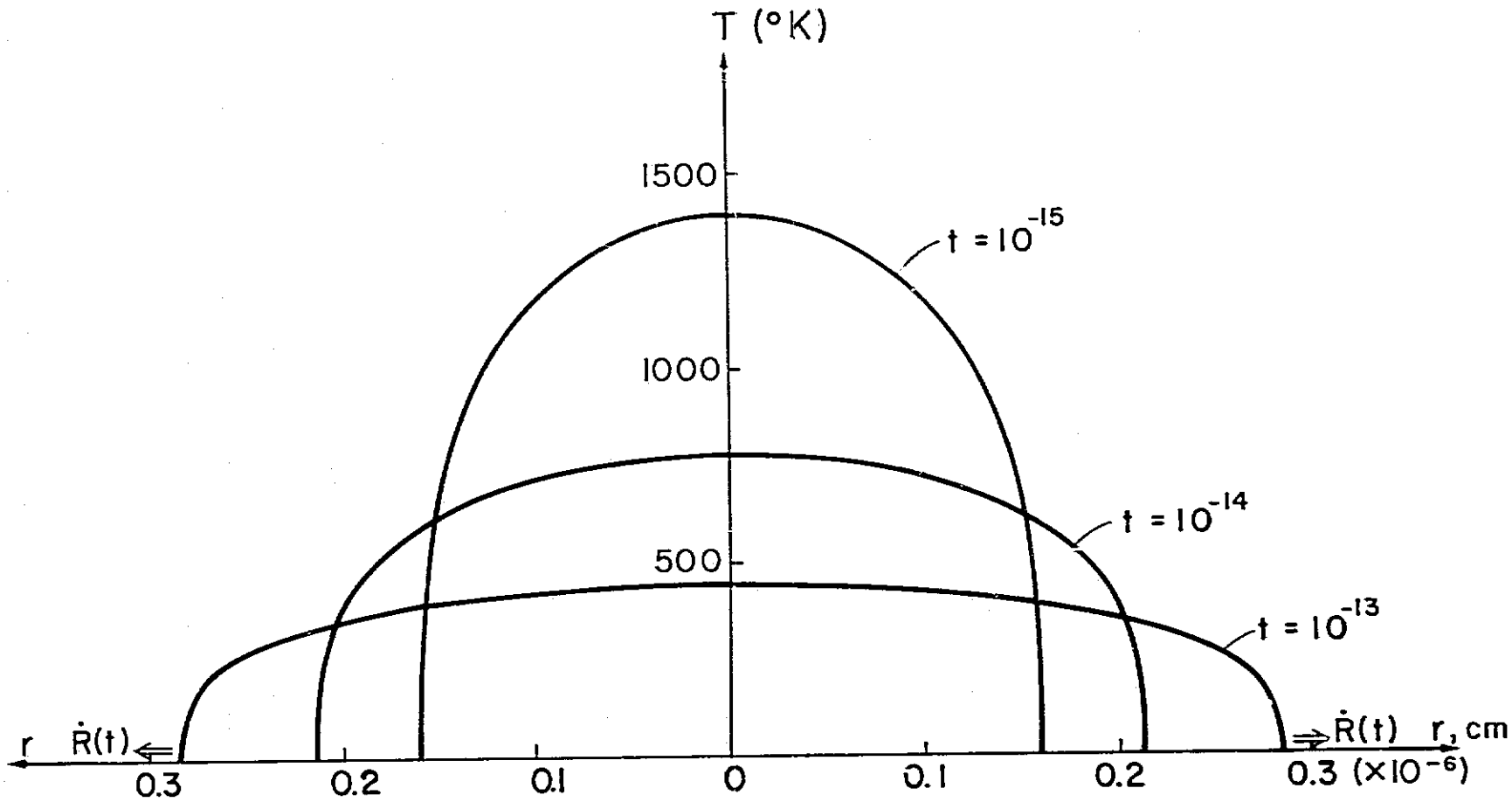

FIG. 1: Parabolic thermal wave in barium oxyde ($\bar{\epsilon} = 10^9$ eV cm^{-1}, $\rho = 5.20$ gr cm^{-3}, $c = 3.57 \times 10^6$ erg gr^{-1}deg^{-1}, $\lambda_o = 3.40 \times 10^{-2}$ erg cm^{-1} sec^{-1}deg^{-4}, $n = 3$).[12-13]

3. HYPERBOLIC THERMAL WAVES

In a transient heat transport process, a temperature gradient produces a heat flow after a finite relaxation period. In accordance with Eqs. (1) - (3), the cylindrical thermal wave generated by an ion of energy ε around its path L in a metal is described by the hyperbolic initial-value problem:

$$\frac{\partial q}{\partial t} = -\frac{1}{\tau} q - \frac{\lambda}{\tau} \frac{\partial T}{\partial r} \quad , \qquad (21)$$

$$\rho c \frac{\partial T}{\partial t} = -\frac{1}{r} \frac{\partial}{\partial r} (rq) \quad , \qquad (22)$$

where

$$2\pi\rho c \int_0^\infty T(r,t)\, r dr = \bar{\varepsilon} \quad . \qquad (23)$$

Sputtering is produced in metals exclusively at temperatures $T > 273^{\circ}K$. In this so-called high temperature region, λ is constant whereas τ is inversely proportional to T [Eq. (5)], i.e.[10]

$$\tau = \tau_o T^{-1}, \qquad [\tau_o] = \text{deg sec} \quad , \qquad (24)$$

$$\lambda = \lambda_o T^0 \ , \qquad [\lambda_o] = \text{erg cm}^{-1} \text{ sec}^{-1} \text{ deg}^{-1} \quad . \qquad (25)$$

Since $[\bar{\varepsilon}/\lambda_o \tau_o] = 0$ and $[\lambda_o/\rho c] = \text{cm}^2\text{sec}^{-1}$, a (nondimensional) similarity variable results from the dimensional parameters $\bar{\varepsilon}$, λ_o, τ_o, ρc and r,t in the form

$$\xi = r/[(\lambda_o/\rho c)t]^{1/2} \quad . \qquad (26)$$

For dimensional reasons ($[\tau_o] = \text{deg sec}$, $[(\lambda_o \rho c)^{1/2} \tau_o] = \text{erg cm}^{-3}$ cm sec^{-1} $\text{sec}^{3/2}$), the temperature and heat flux fields are subject to

the seifsimilar transformations,

$$T(r,t) = \tau_o t^{-1} f(\xi) \quad , \qquad (27)$$

$$q(r,t) = (\lambda_o \rho c)^{1/2} \tau_o t^{-3/2} g(\xi) \quad . \qquad (28)$$

These equations reduce Eqs. (21) - (23) to a problem for ordinary nonlinear differential equations:

$$\xi \frac{dg}{d\xi} + 3g = 2f[g + \frac{df}{d\xi}] \quad , \qquad (29)$$

$$\frac{1}{\xi} \frac{d}{d\xi} (\xi g) = f + \frac{1}{2} \xi \frac{df}{d\xi} \quad , \qquad (30)$$

where

$$2\pi \int_0^\infty f(\xi)\ \xi\ d\xi = e, \qquad e \equiv \bar{\epsilon}/\lambda_o \tau_o \quad , \qquad (31)$$

and $f(\xi)$ and $g(\xi)$ are nondimensional. Eq. (30) is readily integrated,

$$\frac{d}{d\xi} (\xi^2 f - 2\xi g) = 0, \qquad \text{i.e.:} \quad \xi^2 f - 2\xi g = C_o \ ,$$

whence

$$g = \frac{1}{2} \xi f \quad , \qquad (32)$$

since $C_o = 0$ by the condition $g = 0$ for $\xi = 0$[$q(r=0,t) = 0$ for reasons of symmetry]. Elimination of g from Eq. (29) by Eq. (32) yields

$$(\xi^2 - 4f) \frac{df}{d\xi} = 2\xi f(f-2) \quad , \qquad (33)$$

or

$$(\xi^2 - 4f) \frac{df}{d\xi^2} = f(f - 2) \qquad (34)$$

By multiplication with the integrating factor,

$$\mu(f) = f^{-1/2}(f-2)^{-3/2} \quad , \qquad (35)$$

Eq. (34) is transformed into the complete differential,

$$dS(\xi^2,f) = \frac{4f-\xi^2}{f^{1/2}(f-2)^{1/2}}\,df + \frac{f^{1/2}}{(f-2)^{1/2}}\,d\xi^2 = 0 . \qquad (36)$$

Accordingly, the solution $f(\xi)$ is given implicitly, by the integral $S(\xi^2,f) = C$ of Eq. (36):

$$\xi^2 = 8 + [(f-2)/f]^{1/2}\{C - 8\ell n[f^{1/2}+(f-2)^{1/2}]\} \quad . \qquad (37)$$

This result yields directly $\xi = \xi(f)$ and by inversion the solution $f = f(\xi)$, which is symmetrical, $f(+\xi) = f(-\xi)$. In particular, Eq. (37) indicates that a real solution $f(\xi) > 0$ exists only in the interval

$$f_{min} \leq f(\xi) \leq f_{max} \quad \text{for} \quad 8 \geq \xi^2 \geq 0 \quad , \qquad (38)$$

where

$$f = f_{min} = 2 \quad \text{for} \quad \xi = \pm 2\sqrt{2} \quad , \qquad (39)$$

$$f = f_{max} = f_o \quad \text{for} \quad \xi = 0 \quad , \qquad (40)$$

whereas

$$f \equiv 0 \quad \text{for} \quad |\xi| > 2\sqrt{2} \quad , \qquad (41)$$

by Eq. (34), i.e. $f(\xi)$ is discontinuous at $\xi = \pm 2\sqrt{2}$. The value $f_o = f(\xi=0)$ is related through Eq. (37) to the integration constant C,

$$C/8 = \ell n[f_o^{1/2} + (f_o - 2)^{1/2}] - [f_o/(f_o - 2)]^{1/2} \quad . \qquad (42)$$

The energy conservation relation in Eq. (31), which determines C and

thus f_o, becomes

$$\int_{f_o}^{2} f \frac{d\xi^2}{df} df = e/\pi \quad , \qquad (43)$$

by change of the integration variable. Substitution of $d\xi^2/df$ and C in accordance with Eqs. (37) and (42) leads to the transcendental equation,

$$\ell n[f_o^{1/2} + (f_o - 2)^{1/2}] \{\ell n\sqrt{2} + [f_o/(f_o - 2)^{1/2}] - \frac{1}{2} \ell n[f_o^{1/2} + (f_o - 2)^{1/2}]\}$$

$$+ \frac{1}{4}(f_o - 2) - \{[f_o/(f_o - 2)]^{1/2} + \frac{1}{2} \ell n\sqrt{2}\} \ell n\sqrt{2} = e/16\pi \quad , \qquad (44)$$

which gives f_o as the first real root $f_o > 2$. The left side $L(f_o)$ of Eq. (44) assumes the value $L = 0$ for $f_o = 2$ and increases monotonically with increasing $f_o > 2$ so that $L \to \infty$ for $f_o \to \infty$. Hence, a real root $2 < f_o < \infty$ exists for any given $0 < e < \infty$.

It should be noted that the function $f(\xi)$ loses its uniqueness at sufficiently large $e \sim \bar{\varepsilon}$. According to Eq. (37)

$$[df/d\xi^2]_{f = 2 + \varepsilon} = \frac{2\sqrt{2}\, \varepsilon^{1/2}}{C - 8 \ell n\sqrt{2}} \quad , \quad 0 \leq \varepsilon << 1 \qquad . \qquad (45)$$

Hence

$$[df/d\xi^2]_{f = 2 + \varepsilon} \gtrless 0 \quad \text{for} \quad C \gtrless 8 \ell n\sqrt{2} \qquad . \qquad (46)$$

This means that $f(\xi)$ is i) a unique function of ξ^2 for $C < 8 \ell n\sqrt{2}$ but ii) a multivalued function of ξ^2 for $C > 8 \ell n\sqrt{2}$. Since $C = C(f_o)$ [by Eq. (42)] and $f_o = f_o(e) = f_o(\bar{\varepsilon}/\lambda_o \tau_o)$ [by Eq. (44)] increase with increasing f_o and $e \sim \bar{\varepsilon}$, respectively, multivalued thermal flow

appears for $e > \hat{e}$ where

$$C[f_o(\hat{e})] = 8\ \ell n\sqrt{2} \quad . \qquad (47)$$

Accordingly, for an energy release $\bar{\varepsilon} > \hat{\bar{\varepsilon}}$, where the critical value $\hat{\bar{\varepsilon}} = \hat{e}\ \lambda_o \tau_o$ is determined by Eqs. (42), (44), and (47), the energy $\bar{\varepsilon}$ is no longer propagated through an ordinary nonlinear thermal wave but through a thermal shock wave. As expected, thermal shock waves occur at energies $\bar{\varepsilon}$ above a critical value $\hat{\bar{\varepsilon}}$.

By combining the analytical solution $f = f(\xi)$ in Eq. (37) with Eqs. (27) - (28) and (32), one obtains the fields $T(r,t) \sim t^{-1} f(\xi)$ and $q(r,t) \sim t^{-3/2} \xi f(\xi)$ where $\xi \sim r t^{-1/2}$ by Eq. (26). $T(r,t)$ and $q(r,t)$ are decreasing with increasing t at any fixed point $0 < r < r(t)$ within the thermal wave. These fields are discontinuous at the wave front,

$$R(t) = 2\sqrt{2}\ (\lambda_o/\rho c)^{1/2} t^{1/2} \quad , \qquad (48)$$

by Eqs. (20) and (39). The speed of the wave front is

$$\frac{dR(t)}{dt} = \sqrt{2}\ (\lambda_o/\rho c)^{1/2} t^{-1/2} \quad . \qquad (49)$$

Accordingly, the wave spreads out radially with time at a speed decreasing with time. It is interesting that $R(t)$ and $dR(t)/dt$ are independent of $\bar{\varepsilon}$ and τ_o for the particular T - dependence of λ and τ in Eqs. (24) and (25). In this case, $\bar{\varepsilon}$ and τ affect only the height of the distribution $f(\xi)$, i.e. f_o increases with increasing ε and decreasing τ_o [Eq. (44)].

The propagation of a hyperbolic thermal wave in wolfram (W) is shown in Fig. 2 ($m = -1$, $n = 0$). It is seen that the hyperbolic wave exhibits an extremely steep wave front in comparison to the parabolic wave (Fig. 1).

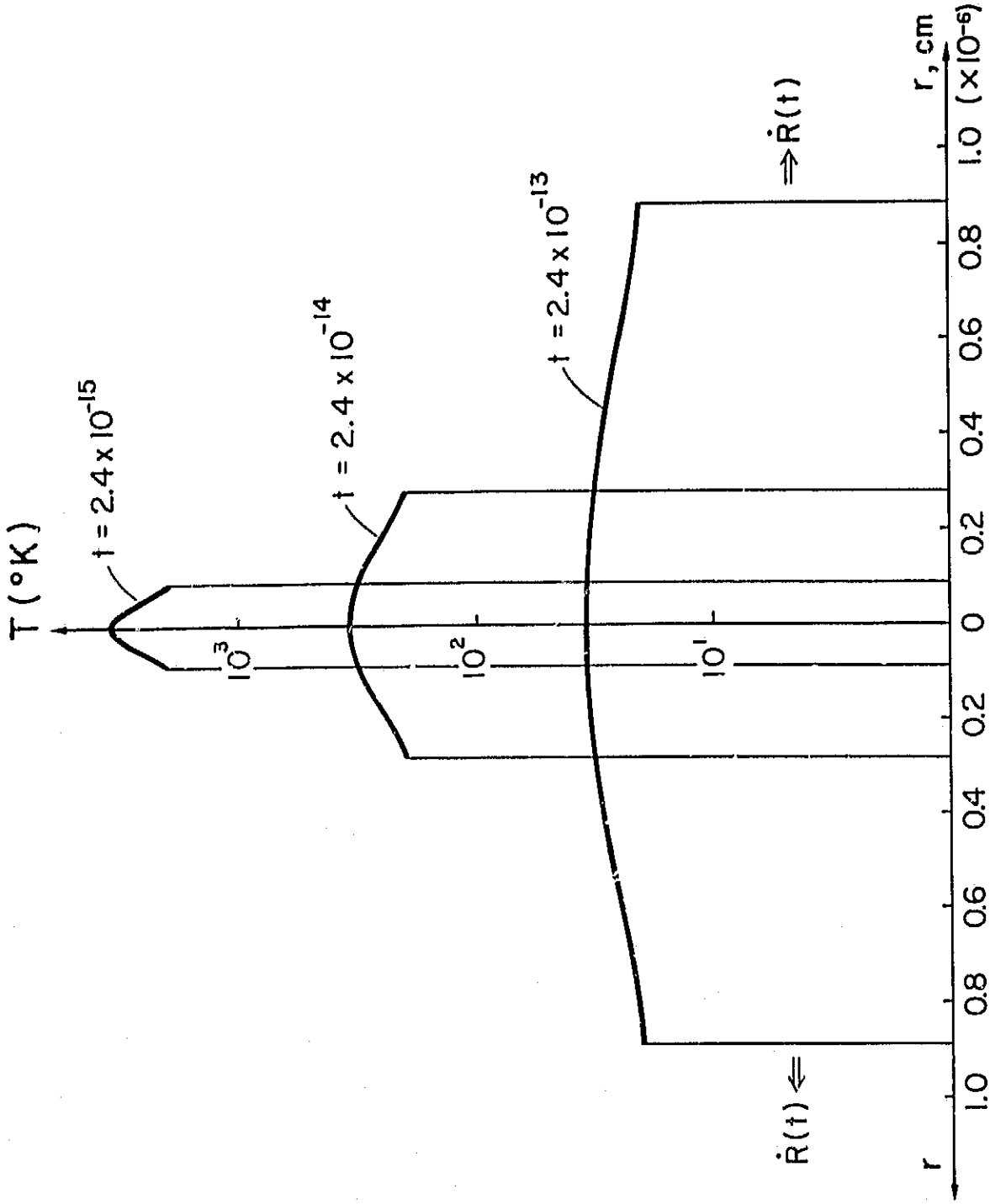

FIG. 2: Hyperbolic thermal wave in wolfram ($\bar{\epsilon} = 10^9$ eV cm^{-1}, $\rho = 19.30$ gr cm^{-3}, $c = 1.51 \times 10^6$ erg gr^{-1} deg^{-1}, $\lambda_o = 1.05 \times 10^7$ erg cm^{-1} sec^{-1} deg^{-1}, $\tau_o = 2.41 \times 10^{-12}$ sec deg, $n = 0$, $m = -1$) [14-15]

4. APPLICATION TO VOLUME SPUTTERING BY IONS

For materials which have a thermal conductivity $\lambda \sim T^n$, $n > 0$, such as metal oxides (e.g. BaO), glasses, graphite, etc., at high temperatures, the parabolic equation gives an approximate description of thermal waves. The parabolic solution [(Eq. 116)] does not indicate the occurrence of shock waves at high ion energies $\bar{\varepsilon}$ and its approximate validity is, therefore, questionable in this energy region. In the case of pure metals, which have a thermal conductivity $\lambda \sim T^0$ and a thermal relaxation time $\tau \sim T^{-1}$, only the hyperbolic system in Eqs. (21) - (22) provides a physically acceptable description of thermal waves. The hyperbolic solution [Eq. (37)] is applicable for ion energies $\bar{\varepsilon} < \hat{\bar{\varepsilon}}$ [Eq. (47)], since it becomes multivalued for $\bar{\varepsilon} > \hat{\bar{\varepsilon}}$ (shock waves).

A thermal wave of cylindrical symmetry represents a first approximation to the actual thermal waves produced by sputtering ions in materials. Deviations from the cylinder symmetry are due to end-effects at the point of impact and the end of the ion path (in particular at low ion energies $\bar{\varepsilon}$), nonuniform slowing down, anisotropies in the directions of the most dense atom arrangement. In these directions, the probability for momentum transfer is largest so that the resulting crater in the material resembles more a cone than a cylinder.

The number of atoms emitted by an ion of given energy $\bar{\varepsilon}$ is mainly determined by the energy conservation equation (whereas the calculation of the spatial distribution of the expelled atoms would require in addition consideration of many-body momentum conservation

in the solid). For this reason, the number of atoms sputtered by an ion may be evaluated macroscopically by means of the thermal wave concept. In this approach, the collective many-body interactions which produce microscopically the thermal energy transfer are contained in the thermal conductivity λ and the relaxation time τ. The crystal bonds of the atoms behind the wave front R are broken so that the atoms are emitted as long as the average particle energy $Mc\bar{T}(t)$ in the thermal wave is larger than the effective threshold energy $\tilde{E}_o$ for sputtering,

$$Mc\bar{T}(t) \equiv 2\pi Mc \int_0^{R(t)} T(r,t)\, r\, dr/\pi R^2(t) \geq \tilde{E}_o,\ \tilde{E}_o = \alpha E_o. \quad (50)$$

where $M = \rho/N$ is the mass of an atom in the solid. The correction factor α takes into consideration that on the average a fraction of the energy $\bar{\varepsilon}$ goes into kinetic energy of the expelled atoms, i.e. in general $1 < \alpha \lesssim 2$. According to experiments, the true sputtering threshold E_o is a material constant which is independent of the mass ratio of the atom and ion.[4-5] The sublimation energy E_s is the energy required on the average for the removal of an atom from the surface of a polycrystalline solid, $E_s = \langle E_s^{ijk} \rangle_{ijk}$ (ijk designates the orientation of the surface). If the atom is expelled from within the solid, then E_o is equal to the dislocation energy E_d of an atom. E_d is the energy required for i) the removal of an atom from its position in the lattice ($\sim 2E_s$) and ii) its stable transfer to an interstitial lattice position ($\sim 2E_s$), i.e. the threshold energy E_o for sputtering is proportional to E_s,

$$E_o = hE_s, \quad h \cong 4 \qquad . \qquad (51)$$

In Table I, the experimentally observed threshold energies E_o for some technically interesting metals[4-5] are compared with the theoretical values following from Eq. (51) for $h = 4$ [note that E_o (experimental) was obtained by independent logarithmic extrapolation of the data in references 4 - 5]. The discrepancies between the experimental and theoretical values of E_o lie well within the experimental uncertainties.

TABLE I. Experimental and Theoretical Threshold Energies.

Metal	E_o(experimental) eV	E_s eV	E_o(theoretical), h=4 eV
Al	16	3.3	13.2
Cu	20	3.5	14.0
Mo	26	6.2	24.8
Ta	35	8.0	32.0
W	36	8.8	35.2

Equation (50) defines a maximum wave front radius within which the crystal bonds of the solid are broken. These atoms are expelled with a relaxation time of the order $t_E \cong \hbar/E_o$. At this phase of the expansion, the thermal wave collapses as its energy ϵ has been consumed in expelling the atoms. According to Eq. (50), $R(\bar{t})$ is given by

$$R(\bar{t}) = [\bar{\epsilon}/\pi\tilde{E}_o(\rho/M)]^{\frac{1}{2}} \qquad (52)$$

for both the parabolic and hyperbolic thermal waves. The number Z of

atoms sputtered by an ion of energy ε is on the average (α)

$$Z = \pi R^2(\bar{t})L(\rho/M)H(\varepsilon - \tilde{E}_o) = (\varepsilon/\tilde{E}_o)H(\varepsilon - \tilde{E}_o) \quad , \qquad (53)$$

$$H(\varepsilon - \tilde{E}_o) = 1, \qquad \varepsilon > \tilde{E}_o \quad ,$$

$$= 0, \qquad \varepsilon < \tilde{E}_o \quad .$$

Equation (53) is based on a discontinuous propagation of the ion energy ε which is provided by the discontinuous thermal wave in the continuum picture ($\varepsilon >> \tilde{E}_o$, $Z >> 1$). Substitution of Eq. (52) into Eqs. (19) and (48) yields the time it takes the parabolic (p) and hyperbolic (h) waves to propagate to the critical radius $R(\bar{t})$,

$$\bar{t}_p = \frac{1}{4\pi}\left(\frac{n}{n+1}\right)^{n+1}\left(\frac{Mc}{\tilde{E}_o}\right)^{n+1}\frac{\bar{\varepsilon}}{\lambda_o} \sim \bar{\varepsilon}/\lambda_o\tilde{E}_o^{n+1} \quad , \qquad (54)$$

$$\bar{t}_h = \frac{1}{8\pi}\frac{Mc}{\tilde{E}_o}\frac{\bar{\varepsilon}}{\lambda_o} \sim \bar{\varepsilon}/\lambda_o\tilde{E}_o \quad . \qquad (55)$$

In applications to ion sputtering, it is to be noted that Eq. (53) is valid for not too large ion energies. At high ion energies, the ion penetrates so far into the solid that only relatively few volume atoms are emitted.

Sputtering by ions with energies significantly larger than the threshold energy ($\varepsilon >> E_o$) occurs at the accelerating grid of ion propulsion devices.[16-17] The velocity distribution of these ions at the surface of the accelerating grid ($z = 0$, $0 \leq r \leq R$) may be simulated by a Gaussian of the form

$$f(\vec{v}) = n(m/2\pi<\varepsilon>)^{3/2}\, e^{-m(\vec{v} - <\vec{v}>)^2/2<\varepsilon>} \qquad (56)$$

where

$n = n(r)$ = ion density at $z = 0,\ 0 \leq r \leq R$

$\langle\varepsilon\rangle = \langle\varepsilon(r)\rangle$ = average random energy at $z = 0,\ 0 \leq r \leq R$

$\langle\vec{v}\rangle = \langle\vec{v}(r)\rangle$ = directed beam velocity at $z = 0,\ 0 \leq r \leq R$

$\vec{v}$ = individual ion velocities relative to grid

If the beam is in thermal equilibrium in its center of mass system then one has $\langle\varepsilon\rangle = kT(r)$. The number of grid atoms sputtered per incident ion of energy $\varepsilon = \frac{1}{2} mv^2$ is by Eq. (53),

$$Z(\tfrac{1}{2} mv^2) = [\tfrac{1}{2} mv^2/\tilde{E}_o]\ H(\tfrac{1}{2} mv^2 - \tilde{E}_o) \quad . \qquad (57)$$

Let θ designate the angle between the vectors $\vec{v}$ and $\langle\vec{v}\rangle$. The number of atoms expelled per unit area of the metal surface and unit time is at the radial location $0 \leq r \leq R$

$$\frac{dN}{dt} = n\left(\frac{m}{2\pi\langle\varepsilon\rangle}\right)^{3/2} \frac{m}{2\tilde{E}_o} *$$

$$* \int_0^{2\pi} \int_0^{\pi/2} \int_{v_o}^{\infty} v^2 e^{-m(\vec{v}-\langle\vec{v}\rangle)^2/2\langle\varepsilon\rangle} (v\cos\theta) v^2 \sin\theta\, d\phi d\theta dv \quad , \qquad (58)$$

$$v_o \equiv (2\tilde{E}_o/m)^{\frac{1}{2}} \quad .$$

After the trivial ϕ-integration and the substitutions,

$$\cos\theta = \tau, \qquad d\tau = -\sin\theta d\theta \quad ,$$

$$\sqrt{\beta}\, v = x, \qquad dx = \sqrt{\beta}\, dv \quad , \qquad (59)$$

and

$$\beta = m/2\langle\varepsilon\rangle, \qquad \gamma = \sqrt{\beta}\ |\langle\vec{v}\rangle| \quad ,$$

$$x_o = \sqrt{\beta}\ (2\tilde{E}_o/m)^{\frac{1}{2}}, \qquad y_o = x_o - \gamma \quad , \qquad (60)$$

Eq. (58) becomes

$$\frac{dN}{dt} = n(m/2\pi\langle\varepsilon\rangle)^{3/2}\ (\pi m/\tilde{E}_o)\beta^{-3}J \quad , \qquad (61)$$

where

$$J = \int_0^1 \int_{x_o}^{\infty} e^{-(x^2 + \gamma^2 - 2\gamma x\tau)} \tau d\tau\ x^5\ dx \quad , \qquad (62)$$

whence

$$J = \tfrac{1}{4}\gamma^{-2}\ e^{-\gamma^2} \int_{x_o}^{\infty} x^3\ e^{-x^2} dx$$

$$+ \tfrac{1}{2}\gamma^{-1} \int_{y_o}^{\infty} (y + \gamma)^4\ e^{-y^2}\ dy$$

$$- \tfrac{1}{4}\gamma^{-2} \int_{y_o}^{\infty} (y + \gamma)^3\ e^{-y^2}\ dy \quad , \qquad (63)$$

i.e.

$$J = \frac{1}{8}\ \gamma^{-2}\ (1 + x_o^2)\ e^{-(x_o^2 + \gamma^2)}$$

$$+ \frac{\sqrt{\pi}}{8}\ \gamma(5 + 2\gamma^2)\ [1 - \Phi(y_o)]$$

$$- \frac{1}{8}\ \gamma^{-2}\ [(1 - 5\gamma^2 - 8\gamma^4) - 12\gamma^3\ y_o$$

$$+ (1 - 8\gamma^2)y_o^2 - 2\gamma y_o^3]\ e^{-y_o^2} \quad . \qquad (64)$$

Since

$$\gamma = (\tfrac{1}{2} m\langle\vec{v}\rangle^2/\langle\varepsilon\rangle)^{\frac{1}{2}}, \qquad x_o = (\tilde{E}_o/\langle\varepsilon\rangle)^{\frac{1}{2}} \quad ,$$

$$y_o = (\tilde{E}_o/\langle\varepsilon\rangle)^{\frac{1}{2}} - (\tfrac{1}{2} m\langle\vec{v}\rangle^2/\langle\varepsilon\rangle)^{\frac{1}{2}} \quad , \qquad (65)$$

one obtains for the number of atoms sputtered per unit area and unit time [Eq. (61)] explicitly:

$$\frac{dN}{dt} = n(2\,\frac{\tfrac{1}{2} m\langle\vec{v}\rangle^2}{\pi m})^{\frac{1}{2}}\, H(\tilde{E}_o,\langle\vec{v}\rangle,\langle\varepsilon\rangle) \qquad (66)$$

where

$$H(\tilde{E}_o,\langle\vec{v}\rangle,\langle\varepsilon\rangle).4(\frac{\tilde{E}_o}{\langle\varepsilon\rangle})(\frac{\tfrac{1}{2} m\langle\vec{v}\rangle^2}{\langle\varepsilon\rangle})^{3/2} = (1 + \frac{\tilde{E}_o}{\langle\varepsilon\rangle})\, e^{-(\tilde{E}_o + \frac{1}{2} m\langle\vec{v}\rangle^2)/\langle\varepsilon\rangle}$$

$$+ \sqrt{\pi}(\tfrac{1}{2} m\langle\vec{v}\rangle^2/\langle\varepsilon\rangle)^{3/2}[5 + 2(\tfrac{1}{2} m\langle\vec{v}\rangle^2/\langle\varepsilon\rangle)]\{1-\Phi[(\frac{\tilde{E}_o}{\langle\varepsilon\rangle})^{\frac{1}{2}} - (\frac{\tfrac{1}{2} m\langle\vec{v}\rangle^2}{\langle\varepsilon\rangle})^{\frac{1}{2}}]\}$$

$$- \{1 - 5(\tfrac{1}{2} m\langle\vec{v}\rangle^2/\langle\varepsilon\rangle)^1 - 8(\tfrac{1}{2} m\langle\vec{v}\rangle^2/\langle\varepsilon\rangle)^2 - 12(\tfrac{1}{2} m\langle\vec{v}\rangle^2/\langle\varepsilon\rangle)^{3/2} \cdot$$

$$\cdot [(\tilde{E}_o/\langle\varepsilon\rangle)^{\frac{1}{2}} - (\tfrac{1}{2} m\langle\vec{v}\rangle^2/\langle\varepsilon\rangle)^{\frac{1}{2}}]^1 + [1 - 8(\tfrac{1}{2} m\langle\vec{v}\rangle^2/\langle\varepsilon\rangle)\,][(\tilde{E}_o/\langle\varepsilon\rangle)^{\frac{1}{2}} -$$

$$(\tfrac{1}{2} m\langle\vec{v}\rangle^2/\langle\varepsilon\rangle)^{\frac{1}{2}}]^2 - 2(\tfrac{1}{2} m\langle\vec{v}\rangle^2/\langle\varepsilon\rangle)^{\frac{1}{2}}\,[(E_o/\langle\varepsilon\rangle)^{\frac{1}{2}} - (\tfrac{1}{2} m\langle\vec{v}\rangle^2/\langle\varepsilon\rangle)^{\frac{1}{2}}]^3\}$$

$$\cdot\, e^{-[(E_o/\langle\varepsilon\rangle)^{\frac{1}{2}} - (\frac{1}{2} m\langle\vec{v}\rangle^2/\langle\varepsilon\rangle)^{\frac{1}{2}}]^2} \qquad . \qquad (67)$$

This result indicates that dN/dt varies in a rather complicated way with increasing $\langle\varepsilon\rangle$, and $\langle\vec{v}\rangle$ for fixed $\tilde{E}_o$. In Fig. 3, $H(\tilde{E}_o,\langle\vec{v}\rangle,\langle\varepsilon\rangle)$ is shown quantitatively in dependence of the energy ratios γ^2 and x_o^2 [Eq. (65)]. With exception of the region of low beam velocities $\langle\vec{v}\rangle$ [compared to the average random velocity $(2\langle\varepsilon\rangle/m)^{\frac{1}{2}}$], i.e. $\gamma^2 \leq 10^{-1}$, $H(\gamma,x_o)$ increases with increasing $\gamma^2 \sim \langle\vec{v}\rangle^2/\varepsilon$ and decreasing $x_o^2 \sim E_o/\varepsilon$.

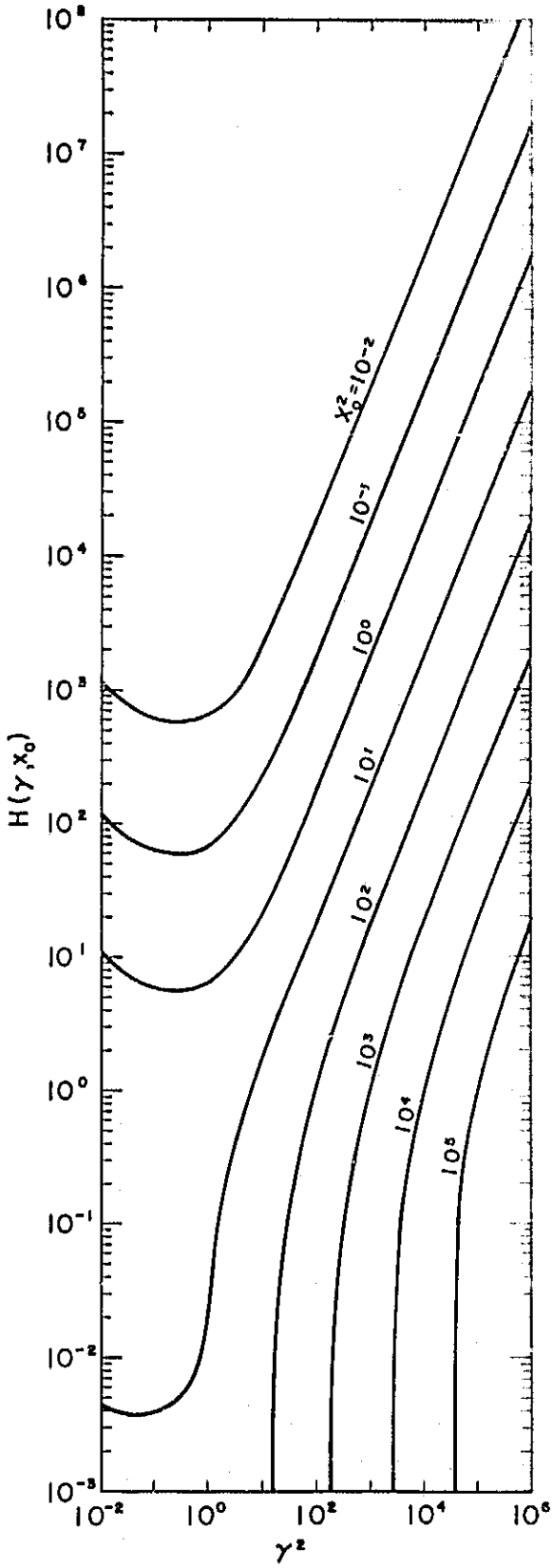

FIG. 3: $H(\gamma, x_0)$ versus γ^2 with x_0^2 as parameter.

5. APPLICATION TO VOLUME SPUTTERING BY MICROMETEORS

The nonlinear thermal wave theory presented explains also the sputtering produced by micrometeors impacting on system components of ion rockets and space ships in general. The above considerations on ion sputtering are transferable to sputtering by micrometeors. In the case of an impinging micrometeor, the energy $\varepsilon = \bar{\varepsilon}L$ [Eqs. (7) and (23)] has to be interpreted as

$$\varepsilon = \tfrac{1}{2} N\bar{m}v^2 \quad , \qquad (68)$$

where $\vec{v}$ is the velocity of the center of mass of the micrometeor, N the number of atoms it is made up of and $\bar{m}$ the average mass,

$$\bar{m} = \frac{1}{N} \sum_{s=1}^{N} N_s m_s \quad . \qquad (69)$$

N_s is the number of atoms of mass m_s contained in the micrometeor. The main chemical components of micrometeors are iron (Fe) or stone (SiO_2).[18] Their speeds v range from 10 km sec^{-1} to 10^4 km sec^{-1}.[18] The radii of micrometeors range from $r_{min} \cong 10^{-6}$ cm to $r_{max} \cong 10^{-1}$ cm, and their mass per volume of space greatly exceeds that of all other meteors[18] ($r \gtrsim 10^{-1}$ cm). For this reason, micrometeors are most likely to hit ion rockets and space ships outside of the atmosphere of the planets. For micrometeors, the effective sputtering threshold is about [Eqs. (50) - (51)]

$$\bar{E}_o = \alpha E_o = \alpha 4 E_s \cong 8E_s \quad , \qquad (70)$$

i.e. eight times the sublimation energy E_s. The sublimation energy is $E_s/\bar{m} = 7 \times 10^{10}$ erg/gr for Fe and $E_s/\bar{m} \cong 14 \times 10^{10}$ erg/gr (including

dissociation energy) for SiO_2. According to Eq. (70), the critical minimum speed for a micrometeor to vaporize itself on impact is

$$v_{min} = (2\,\tilde{E}_o/\bar{m})^{1/2} \quad . \qquad (71)$$

Hence, $v_{min} \cong (2 \times 8 \times 7 \times 10^{10})^{1/2} \cong 10^6$ cm sec^{-1} = 10 km sec^{-1} for a pure Fe-micrometeor, and $v_{min} \cong (2 \times 8 \times 14 \times 10^{10})^{1/2} \cong 1.5 \times 10^6$ cm sec^{-1} = 15 km sec^{-1} for a pure SiO_2-micrometeor. In order that the thermal wave vaporizes also a significant volume of the material of the system on which the micrometeor impacted, the speed of the latter must satisfy the basic inequality

$$v >> v_{min} \quad . \qquad (72)$$

As the above examples indicate, this condition is satisfied for a significant percentage of micrometeors which have speeds $v = 10^2$ km sec^{-1} and larger (note that the sublimation energies E_s of all solid materials are of the same magnitude-of-order, i.e. a few electron volts). The number of atoms Z sputtered by a micrometeor with a speed $v >> v_{min}$ out of the target material is [Eq. (53)]

$$Z = \varepsilon/\tilde{E}_o = \tfrac{1}{2}N\bar{m}v^2/\tilde{E}_o \quad . \qquad (73)$$

For a Fe-micrometeor of radius $r = 10^{-4}$ cm and speed $v = 10^8$ cm sec^{-1}, one has $\varepsilon = \tfrac{1}{2}(4\pi r^3/3)\bar{m}v^2/\Delta \cong 2 \times 10^{-12}\ 9.3 \times 10^{-23}\ 10^{16}/10^{-23} \cong 2 \times 10^5$ erg (atomic volume $\Delta \cong 10^{-23}$ cm^3). On a wolfram target ($E_o = 35$ eV, $\tilde{E}_o = 8 \times 35 \times 1.6 \times 10^{-12} \cong 3 \times 10^{-10}$ erg), this micrometeor would sputter $Z = \varepsilon/\tilde{E}_o = 2 \times 10^5/3 \times 10^{-10} \cong 10^{15}$ atoms. The corresponding sputtering crater has an extension of the order $\bar{R} \cong (Z\Delta)^{1/3} = (10^{15} \times 10^{-23})^{1/3} = 2 \times 10^{-3}$ cm.

The formulas derived for thermal waves and volume sputtering in sections I, 3-5 are similarly applicable to the unloading and sputtering by micrometeors. The necessary modifications are defined in Eqs. (68) - (73).

References

1. A. von Hippel, Ann. d. Physik 80, 672 (1926); 81, 1043 (1925).

2. C. H. Townes, Phys. Rev. 65, 319 (1944).

3. G. Leibfried, Lattice Theory of Mechanical and Thermal Properties of Matter, Handbook of Physics VII, 1, Springer-Verlag, Berlin 1955.

4. R. V. Stuart and G. K. Wehner, J. Appl. Phys. 33, 2345 (1962).

5. Sh. G. Askerov and L. A. Sena, Sov. Phys. - Solid State 11, 1288 (1969).

6. E. S. Lamar and K. T. Compton, Science 80, 541 (1934).

7. D. E. Harrison and G. D. Magnuson, Phys. Rev. 122, 1421 (1961).

8. For a general review, see M. Kaminsky, Atomic and Ionic Impact Phenomena on Metal Surfaces, Academic Press, New York 1965.

9. N. F. Mott and H. S. W. Massey, The Theory of Atomic Collisions, At the Clarendon Press, Oxford 1965.

10. H. Jones, Theory of Electrical and Thermal Conductivity in Metals, Handbook of Physics XIX, Springer-Verlag, New York 1956.

11. Ya. B. Zeldovich and Yu. P. Raizer, Physics of Shock Waves and High Temperature Hydrodynamic Phenomena, Academic Press, New York 1967.

12. B. H. Billings et al, American Institute of Physics Handbook, McGraw-Hill, New York 1972.

13. Y. S. Touloukian et al, Thermophysical Properties of Matter (The TPRC Data Series), Vol. 2 and Vol. 5, Purdue University 1970.

14. F. Kohlraush, Practical Physics, III, B. G. Teubner, Stuttgart 1968.

15. H. Westphely, Thermal Conductivity of Metals and Alloys, in Landolt-Boernstein, Vol. 4, Part 4, Springer-Verlag, New York, 1972.

16. J. F. Staggs, W. P. Gula, and W. R. Kerslake, J. Spacecraft 5, 159 (1968).

17. D. D. Beebe, S. Nakanishi, and R. C. Rinke, NASA TM X-3044 (1974).

18. E. J. Oepik, Physics of Meteor Flight in the Atmosphere, Interscience Publ., New York 1958.

II. CONTRIBUTIONS TO SURFACE SPUTTERING

At sufficiently low energies of the incident ions, exclusively surface atoms of the solid are sputtered. The experimental data on sputtering of metal surfaces indicate that the average number $S(E)$ of atoms sputtered per incident ion of energy E lies in the interval[1)]

$$0 \leq S(E) < 1, \qquad E_o \leq E < 10^2 \text{ eV} \qquad ,$$

where E_o is the threshold energy for sputtering of surface atoms. The measured $S(E)$ - curves can be fitted by analytical expressions of the form[2)]

$$S(E) = a(E - E_o)^n, \qquad a = \text{const}, \; n = 2 \qquad ,$$

at low energies, $E_o \leq E < 10^2$ eV. It is shown that this simple sputtering formula can be explained theoretically by means of a 3-body sputtering mechanism involving the ion and two surface atoms of the solid. By means of a statistical analysis and a quantum mechanical perturbation theory one finds independently that $n=2$ and that "a" is a weak function of energy E which can be taken to be a constant for $E \gtrsim E_o$, i.e. $a(E) \cong a(E_o)$.

An ordinary binary collision between a surface atom of the solid and an ion incident normal to the surface can evidently not lead to sputtering since the atom does not acquire a momentum component in the direction of the external normal of the surface. Similarly, sputtering is not likely to occur for smaller angles of ion incidence if its energy is not large compared to the threshold energy for sputtering.

It is evident that sputtering, at ion energies of the order of the threshold energy, is a 3-body process involving one ion and two surface atoms of the solid. At higher ion energies, however, sputtering will result mainly from higher order many-body interactions.

By restricting the theoretical considerations to ion energies E of the order of the threshold energy E_o, $E_o \leq E < 10^2$ eV, sputtering is regarded as the result of an ion-atom-atom interaction. Furthermore, it is assumed that the solid is polycrystalline and has a sublimination energy which is on the average $E_s = < E_s^{ijk} >$ where the average is taken over the randomly distributed surfaces (ijk) of the crystallites. In this case, the sublimation energy E_s represents the average binding energy of a surface atom. In the 3-body sputtering process, the ion transfers i) the energy E_s to the atom which is expelled and ii) the energy $2E_s$ or $4E_s$ to the other atom depending on whether the latter is pushed to an unstable or stable interstitial lattice position, as well as iii) kinetic energy. Accordingly, the average sputtering threshold should be

$$E_o = \tfrac{1}{2} (E_s + 2E_s; + E_s + 4E_s) = 4E_s \qquad (1)$$

In experiments which cannot detect individual but only a large number of sputtering events (e.g. sputtering of glow discharge cathodes and accelerating grids), the threshold E_o represents always an average value, i.e. not the absolute smallest possible binding energy of a surface atom which can be as small as $E_s^{ijk}/5$ where $i'j'k'$ designates that surface which has the smallest sublimation energy. It is interesting that the (average) threshold for surface sputtering is

equal to the threshold for volume sputtering since the energy for stable displacement of an atom within the solid is also $4E_s$.

When an ion of low energy as defined above hits the surface of a solid, one of the following processes may occur: 1) the ion is reflected without energy loss by the bound surface atom it encounters; 2) the ion collides with a surface atom and quasi-simultaneously with a second atom so that 3-body sputtering results. (More precisely, the designation "atom" should be used for the incident "ion" since the latter certainly recombines with an electron as it approaches the surface of the solid.) The total probability for the ion to interact in either of the two ways with the solid is

$$P_N = N^{2/3}\sigma(E) \qquad (2)$$

where N is the number density of atoms in the solid and $\sigma(E)$ is the (energy dependent) cross section for ion-atom scattering. Let $W_1(E)$ and $W_2(E)$ be the probabilities for the processes 1) and 2), respectively. The relative probability with which sputtering occurs is then

$$W_s(E) = \frac{W_2(E)}{W_1(E) + W_2(E)} \simeq \frac{W_2(E)}{W_1(E)}\ , \quad W_2(E) \ll W_1(E). \qquad (3)$$

Combining of Eqs. (2) and (3) yields for the sputtering rate, i.e. the number of atoms expelled on the average by one ion of energy E from the solid,

$$S(E) = \sigma(E)N^{2/3}\ W_s(E) \qquad . \qquad (4)$$

For the evaluation of $W_s(E)$, two methods, which are based on different approximations, will be used. The total cross section

$\sigma(E)$ is assumed to be known either theoretically or experimentally.[3-4] One of the methods holds in the case that the interaction by the ion can be treated as a perturbation, whereas the other method holds for arbitrary strong interactions but assumes quantum-statistical equilibrium among the final sputtering states. The latter assumption appears to be questionable at first sight since the small energy region under consideration permits only a relative small number of final states. As a justification it is noted that these different approaches lead essentially to the same result.

1. STATISTICAL ANALYSIS

The basic assumption is made that the final sputtering states correspond to a quantum statistical equilibrium brought about by the strong interaction between the ion and the surface atoms. In the processes 1) or 2), the ion interacts with the surface of the solid within an area of the extension of the de Broglie wavelength, $\lambda = \hbar/\sqrt{2mE}$. For this reason, the spatial part of the phase space is taken to be[5)]

$$V = \frac{4\pi}{3} R^3, \quad R \tilde{=} \hbar/(2mE)^{\frac{1}{2}} \qquad . \qquad (5)$$

In quantum-statistical equilibrium, the probability for transition into a final state is proportional to i) the probability that the interacting particles are simultaneously within V and ii) the density of final states $d\rho/dE$ per unit energy. For a state containing n independent particles with momenta $\vec{p}_1, \vec{p}_2, \ldots, \vec{p}_n$, w and $d\rho/dE$ are given by

$$w = (\frac{V}{\Omega})^n, \qquad \frac{d\rho}{dE} = [\frac{\Omega}{(2\pi\hbar)^3}]^n \frac{d\Phi(E)}{dE} \qquad . \qquad (6)$$

Ω designates the normalization volume, $\Omega > V$, and $\Phi(E)$ is the volume of momentum space corresponding to the total energy E. Accordingly, the probability for transition into the final state n under consideration is

$$W(E) = [V/(2\pi\hbar)^3]^n \frac{d\Phi(E)}{dE} \qquad . \qquad (7)$$

This equation represents the basis for the determination of the process probabilities $W_1(E)$ and $W_2(E)$. Because of the conservation

laws, the n particles in the interactions 1) and 2) are not independent. This requires certain modifications of Eq. (7) which are explained in the applications below.

$W_1(E)$ is defined as the probability for the ion to be reflected at the surface of the solid without energy loss. In the center of mass system (solid), the ion momentum is $p = \sqrt{2mE}$ in the final state and the momentum space volume is $\Phi(E) = 4\pi p^3/3$. According to Eq. (7), the probability for reflection is (n=1)

$$W_1(E) = [V/(2\pi\hbar)^3]^1 \; 4\pi\sqrt{2}m^{3/2} \; E^{1/2} \quad . \qquad (8)$$

$W_2(E)$ is defined as the probability for the 3-body sputtering state. In the center of mass system, the momenta of the ion (i), the sputtered atom (s), and the second atom (a) can be chosen as

$$\vec{p}_i = \vec{p}, \; \vec{p}_s = -\frac{1}{2}\vec{p} - \vec{q}, \quad p_a = -\frac{1}{2}\vec{p} + \vec{q} \quad , \qquad (9)$$

so that momentum is conserved $\Sigma_j \vec{p}_j = \vec{0}$. Since the energy E_o [Eq. (1)] is expended in the sputtering interaction, the total kinetic energy of the three particles is

$$E^* = E - E_o = (\frac{1}{2m} + \frac{1}{4M})\vec{p}^2 + \frac{1}{M}\vec{q}^2 \quad . \qquad (10)$$

Equation (10) represents an ellipsoid with the axes sections $\{[mM/(m + 2M)]E^*\}^{1/2}$ and $(ME^*)^{1/2}$ in the six-dimensional space of the vectors $\vec{p}$ and $\vec{q}$. Hence, the volume of the momentum space is

$$\Phi(E) = \frac{\pi^3}{6}(\frac{4mM^2}{m + 2M})^{3/2} \; E^{*3} \quad . \qquad (11)$$

Owing to conservation of momentum, only two of the particle momenta are independent, i.e. n=2. Substitution of Eq. (11) into Eq. (7) gives for the probability of the sputtering state

$$W_2(E) = [V/(2\pi\hbar)^3]^2 \, 4\pi^3 \left(\frac{mM^2}{m + 2M}\right)^{3/2} E^{*2} \quad , \qquad (12)$$

With the assumption $W_1(E) >> W_2(E)$, one obtains from Eqs. (5) (8), and (12) for the relative sputtering probability the approximate expression

$$W_s(E) \simeq \frac{1}{2\pi} \left[\frac{(M/m)^2}{1 + 2(M/m)}\right]^{3/2} \frac{(E - E_o)^2}{E^2} \qquad (13)$$

where V has been eliminated in accordance with Eq. (5).

2. PERTURBATION THEORY

If the interaction energy between the ion and the surface atoms is sufficiently small, 1) the reflection of the ion by a surface atom without energy loss, and 2) the 3-body ion-atom-atom sputtering with an energy loss $E > E_o$ may be treated by perturbation theory. The probability rates for these processes are most conveniently determined by means of Fermi's Golden Rule.[6]

In the case of the ion reflection, the magnitude of the momentum after the collision is $p = \sqrt{2mE}$ in the center of mass system. The probability per unit time of the reflection transition is

$$w_1(E) = \frac{2\pi}{\hbar} |M_{if}^{(1)}|^2 \frac{d\rho}{dE} \tag{14}$$

where

$$M_{if}^{(1)} = \iiint_{\Omega} \psi_f^* \tilde{H} \psi_i \, d^3\vec{r}$$

and

$$\frac{d\rho}{dE} = [\Omega/(2\pi\hbar)^3] \, 2\pi\sqrt{2}m^{3/2} \, E^{1/2} \tag{16}$$

are the matrix element of the perturbation $\tilde{H}_1$ (operator) in the Hamiltonian of the ion-atom system which causes the transition $i \to f$ and the density of final states per unit energy, respectively. ψ_i and ψ_f are the wave functions of the total system before and after the transition which are normalized for the volume Ω. According to Eqs. (14) - (16), the probability for the ion reflections is per unit time

$$w_1(E) = \frac{2\pi}{\hbar} [\Omega/(2\pi\hbar)^3]^1 |M_{if}^{(1)}|^2 4\pi\sqrt{2}m^{3/2} \, E^{1/2} \quad . \tag{17}$$

The final state of the sputtering interaction consists of an ion of momentum $\vec{p}_i = \vec{p}$, a sputtered atom of momentum $\vec{p}_s = -\frac{1}{2}\vec{p} - \vec{q}$, and a displaced surface atom of momentum $\vec{p}_a = -\frac{1}{2}\vec{p} + \vec{q}$ in the center of mass system. Since $\Sigma_j \vec{p}_j = \vec{0}$, only two particle momenta are independent which determine the statistics. The probability per unit time of the sputtering transition is

$$w_2(E) = \frac{2\pi}{\hbar} |M_{if}^{(2)}|^2 \frac{d\rho}{dE} \tag{18}$$

where

$$M_{if}^{(2)} = \iiint_{\Omega} \psi_f^* \tilde{H}_2 \psi_i \, d^{3}\vec{r} \tag{19}$$

and

$$\frac{d\rho}{dE} = [\Omega/(2\pi\hbar)^3]^2 4\pi^3 \left(\frac{mM^2}{m + 2M}\right)^{3/2} (E - E_o)^2 \quad . \tag{20}$$

ψ_i and ψ_f are the wave functions of the system consisting of the ion and the two surface atoms before and after sputtering, respectively. $\tilde{H}_2$ is the perturbation (operator) in the Hamiltonian of the 3-body system which causes the transition $i \to f$. Equation (20) gives the density of final states per unit energy for the normalization volume Ω. From Eqs. (18) - (20) results the probability for the sputtering transition per unit time,

$$w_2(E) = \frac{2\pi}{\hbar} [\Omega/(2\pi\hbar)^3]^2 |M_{if}^{(2)}|^2 4\pi^3 \left(\frac{mM^2}{m + 2M}\right)^{3/2} (E - E_o)^2. \tag{21}$$

With the assumption $w_2(E) \ll w_1(E)$, one obtains from Eqs. (3), (17) and (21) for the relative sputtering probability the approximate expression

$$W_s(E) = \frac{\Omega}{8\pi\sqrt{2}} \frac{|M_{if}^{(2)}|^2}{|M_{if}^{(1)}|^2} \left(\frac{M^2}{m + 2M}\right)^{3/2} \frac{(E - E_o)^2}{E^{1/2}} \quad . \qquad (22)$$

Since sputtering is a 3-body while reflection is a 2-body interaction, the ratio,

$$|M_{if}^{(2)}|^2 / |M_{if}^{(1)}|^2 \cong H_{21}^2 \, \tilde{\Omega}/\Omega \quad , \qquad (23)$$

is essentially the probability $w = \tilde{\Omega}/\Omega$ for finding one surface atom within the interaction volume

$$\tilde{\Omega} \cong \frac{4\pi}{3} (\hbar^2/2mE)^{3/2} \quad , \qquad (24)$$

the radius of which is of the order of the de Broglie wave length of the incident ion. Accordingly, the relative sputtering probability in Eq. (22) can be written as

$$W_s(E) \cong \frac{H_{21}^2}{24} \left[\frac{(M/m)^2}{1 + 2(M/m)}\right]^{3/2} \frac{(E - E_o)^2}{E^2} \quad . \qquad (25)$$

The determination of the factor $H_{21} \sim 1$, which may be weakly energy dependent, requires introduction of an appropriate interaction potential and a detailed evaluation of the matrix elements.

3. SURFACE SPUTTERING RATE

In 1) and 2) it has been demonstrated that the statistical method [Eq. (13)] and the perturbation approach [Eq. (25)] lead to practically the same relative probability for sputtering $W_s(E)$. Combining this result with Eq. (4) yields for the sputtering rate the formula:

$$S(E) \cong \frac{H_{21}^2}{24}\,\sigma(E)N^{2/3}\left[\frac{(M/m)^2}{1+2(M/m)}\right]^{3/2}\frac{(E-E_o)^2}{E^2} \quad . \qquad (26)$$

Since $E_o = 4E_s \cong 12 - 35$ eV for various metals and $E \gtrsim E_o$ for low energy sputtering, Eq. (26) can be simplified to

$$S(E) \cong \frac{H_{21}^2}{24}\,\sigma(E_o)N^{2/3}\left[\frac{(M/m)^2}{1+2(M/m)}\right]^{3/2}\frac{(E-E_o)^2}{E_o^2} \quad . \qquad (27)$$

In the considerations under 1), 2), and 3), the effect of the particle spin I on the various probabilities has not been included explicitly for reasons of a simple notation. In cases where the ion and surface atoms have no spin, $I_i = I_s = 0$, or the same spin, $I_i = I_s \neq 0$, no corrections arise in the expression for $W_s(E)$ and $S(E)$. In case of different spins, $I_i \neq I_s$, $W_s(E)$ and $S(E)$ are increased by the factor (statistical spin weight)

$$g_s = 2I_s + 1 \quad . \qquad (28)$$

Equation (27) is exactly of the form of the phenomenological expression found by analytically fitting the experimental data.[1-2] According to the more general Eq. (25), $S(E)$ reaches with increasing E a plateau-like maximum and decreases then since $\sigma(E)$ decreases at sufficiently high energies E. Thus, Eq. (26) appears to be correct

not only in the low energy region $E \gtrsim E_o$, but seems to agree also at high energies $E >> E_o$ qualitatively with the experimental sputtering curves.[1-2)]

It is noted that the particular energy dependence $\sim(E - E_o)^2/E^2$ in Eq. (26) is due to the 3-body interaction which has been assumed to be th essential mechanism in low energy surface sputtering. At higher ion energies, higher-order many body interactions are energetically possible so that not only surface but also an increasing number of volume atoms are sputtered $(S(E) > 1)$.

4. APPLICATION TO ELECTRICAL DISCHARGE SPUTTERING

In low pressure discharges, such as glow discharges, practically the entire external voltage U_o drops across the cathode sheath λ. In this region, the discharge ions, which have a thermal velocity distribution at the temperature $T \cong T_e$ if the sheath is stable, are accelerated to a mean velocity $\langle\vec{v}\rangle$. The resulting quasi-thermal ion beam bombards the cathode, which emits atoms in accordance with Eq. (26). Since the cathode drop is of the order $\Delta U = 20 - 30$ volt, the unidirectional ion beam energy is frequently smaller than the sputtering threshold, $e\Delta U < E_o$. For this reason, it is essential to take into consideration the thermal velocity distribution of the ions. Mainly the ions of the tail of the velocity distribution cause sputtering of the cathode in this case.

The cathode sputtering in low pressure discharges is a process caused by ions of low energy, $E \gtrsim E_o$. Accordingly, the number of atoms sputtered on the average by an ion incident with the energy $E = \frac{1}{2} mv^2$ is given by Eq. (26),

$$S(\tfrac{1}{2} mv^2) = a(\tfrac{1}{2} mv^2 - E_o)^2 \quad , \qquad (29)$$

$$a \equiv \sigma(E_o) N^{2/3} \frac{H_{21}^{\,2}}{24} \left[\frac{(M/m)^2}{1 + 2(M/m)}\right]^{3/2} E_o^{-2} \quad . \qquad (30)$$

The velocity distribution of the ions, which arrive with the mean velocity $\langle\vec{v}\rangle$ at the cathode, is assumed to be a Maxwellian in the beam system, i.e.

$$f(\vec{v}) = n(m/2\pi kT)^{3/2} \, e^{-m(\vec{v} - \langle\vec{v}\rangle)^2/2kT} \qquad (31)$$

where $\vec{v}$ designates the individual velocities of the ions in the system of the discharge, and n and T are the density and temperature of the ions, respectively.

The ion beam velocity $\langle\vec{v}\rangle$ is determined by the electric field $\vec{F}$ in the cathode sheath which is, according to probe measurements,[7] a linear function of the axial discharge coordinate z,

$$F(z) = \hat{F}(1 - \frac{z}{\lambda}), \qquad \hat{F} \cong 2\, U_o/\lambda \quad , \qquad (32)$$

where λ is the extension of the sheath and U_o is the external voltage. The potential difference across the sheath is

$$\Delta U = \hat{F}\lambda/2 \cong U_o \quad . \qquad (33)$$

Since collisions involving ions represent a small effect, the magnitude of the ion beam velocity at the cathode is in good approximation given by

$$|\langle\vec{v}\rangle| = (2e\Delta U/m)^{1/2} \cong (2eU_o/m)^{1/2} \quad . \qquad (34)$$

The ions within the cone $0 \leq \theta \leq \pi/2$ [$\theta \nless (\vec{v}, \langle\vec{v}\rangle)$] which are at a distance $\Delta z = v\cos\theta\,\Delta t$ from the cathode, strike the latter within unit time $\Delta t = 1$. Accordingly, the number of atoms sputtered per unit surface area and unit time out of the cathode is

$$\frac{dN}{dt} = an\,(\frac{m}{2\pi kT})^{3/2} \int_0^{2\pi}\int_0^{\pi/2}\int_{v_o}^{\infty} e^{-m(\vec{v} - \langle\vec{v}\rangle)^2/2kT}$$

$$*(\tfrac{1}{2}mv^2 - E_o)^2(v\cos\theta)v^2 \sin\theta\, d\phi\, d\theta\, dv \quad ,$$

$$v_o \cong (2E_o/m)^{1/2} \quad , \qquad (35)$$

by Eqs. (29) - (31). By means of the substitutions,

$$\cos\theta = \tau, \qquad d\tau = -\sin\theta\, d\theta \quad ,$$

$$\sqrt{\beta}v = x, \qquad dx = \sqrt{\beta}dv \quad , \tag{36}$$

and

$$\beta = m/2kT, \qquad \gamma = \sqrt{\beta}\,|\langle\vec{v}\rangle| \quad ,$$

$$x_o = \sqrt{\beta}(2E_o/m)^{1/2}, \quad y_o = x_o - \gamma \quad , \tag{37}$$

Eq. (35) is transformed to

$$\frac{dN}{dt} = 2\pi an\left(\frac{m}{2\pi kT}\right)^{3/2}\beta^{-2}\left[J_0(E_o,\langle\vec{v}\rangle,T)\,E_o^{\,2} - J_1(E_o,\langle\vec{v}\rangle,T)\,m\beta^{-1}E_o\right.$$

$$\left. + J_2(E_o,\langle\vec{v}\rangle,T)\left(\frac{m}{2}\beta^{-1}\right)^2\right] \tag{38}$$

where

$$J_n(E_o,\langle\vec{v}\rangle,T) = \int_0^1\int_{x_o}^{\infty} x^{3+2n}\, e^{-(x^2+\gamma^2-2\gamma x\tau)}\,\tau d\tau\, dx, \tag{39}$$

with $n = 0,1,2$. The τ-integration reduces this double integral to

$$J_n(E_o,\langle\vec{v}\rangle,T) = \frac{e^{-\gamma^2}}{4\gamma^2}\int_{x_o}^{\infty} x^{1+2n}\, e^{-x^2}\, dx$$

$$+ \frac{1}{2\gamma}\int_{y_o}^{\infty}(y+\gamma)^{2(1+n)}\, e^{-y^2}\, dy$$

$$- \frac{1}{4\gamma^2}\int_{y_o}^{\infty}(y+\gamma)^{1+2n}\, e^{-y^2}\, dy \quad . \tag{40}$$

Upon a binomial expansion and evaluation of the resulting integrals*) in Eq. (40), there follows:

$$J_0(E_o,\langle\vec{v}\rangle,T) = \frac{\gamma^{-2}}{8} e^{-(x_o^2+\gamma^2)} + \frac{\sqrt{\pi}}{4}[1-\Phi(y_o)] - \frac{\gamma^{-2}}{8}[(1-4\gamma^2)-2\gamma y_o] e^{-y_o^2}, \quad (41)$$

$$J_1(E_o,\langle\vec{v}\rangle,T) = \frac{\gamma^{-2}}{8}(1+x_o^2) e^{-(x_o^2+\gamma^2)} + \frac{\sqrt{\pi}}{8}\gamma(5+2\gamma^2)[1-\Phi(y_o)] - \frac{\gamma^{-2}}{8}[(1-5\gamma^2-8\gamma^4)-12\gamma^3 y_o+(1-8\gamma^2)y_o-2\gamma y_o^3] e^{-y_o^2}, \quad (42)$$

$$J_2(E_o,\langle\vec{v}\rangle,T) = \frac{\gamma^{-2}}{8}(2+2x_o^2+x_o^4) e^{-(x_o^2+\gamma^2)} + \frac{\sqrt{\pi}}{16}\gamma(35+28\gamma^2+4\gamma^4)[1-\Phi(y_o)] + \frac{\gamma^{-2}}{8}[(-2+14\gamma^2+35\gamma^4+12\gamma^6) + (35\gamma^2+30\gamma^5)y_o + (-2+14\gamma^2+40\gamma^4)y_o^2 + 30\gamma^3 y_o^3 + (-1+12\gamma^2)y_o^4 + 2\gamma y_o^5] e^{-y_o^2}. \quad (43)$$

---

*) In accordance with

$$\int x^n e^{-x^2} dx = -e^{-x^2}\sum_{m=0}^{r-1}(n-1;-2;m)2^{-(1+m)}x^{n-2m-1} + (1-s)(1;2;r)2^{-(1+r)}\sqrt{\pi}\,\Phi(x) + \text{const}$$

where $(n;d;m) = n(n+1d)(n+2d)\ldots[n+(m-1)d]$ and $n = 2r-s$ with $s = 0$ or $s = 1$.

where

$$\phi(y) = \equiv \frac{2}{\sqrt{\pi}} \int_0^y e^{-x^2} dx = \frac{2}{\sqrt{\pi}} \sum_{m=0}^{\infty} (-1)^m \, y^{2m+1}/(2m+1)m! \tag{44}$$

is the error function. Substitution of Eqs. (41) - (43) into Eq. (38) leads to the final expression for the number of atoms sputtered per unit surface area and unit time from the cathode:

$$\frac{dN}{dt} = an\left(\frac{\langle v\rangle^2}{\pi}\right)^{1/2} E_o^2 \, \Lambda(E_o, \langle\vec{v}\rangle, T) \tag{45}$$

where

$$\begin{aligned}\Lambda(E_o, \langle\vec{v}\rangle, T) = {} & \frac{\gamma^{-3}}{4}\left[1 - 2(1 + x_o^2)\, x_o^{-2} + (2 + 2x_o^2 + x_o^4)\, x_o^{-4}\right] e^{-(x_o^2+\gamma^2)} \\ & + \frac{\sqrt{\pi}}{2}\left[1 - (5 + 2\gamma^2)\, x_o^{-2} + \frac{1}{4}(35 + 28\gamma^2 + 4\gamma^4)\, x_o^{-4}\right]\left[1 - \Phi(y_o)\right] \\ & + \frac{\gamma^{-3}}{4}\{(-1 + 4\gamma^2 + 2\gamma y_o) \\ & + 2\left[(1 - 5\gamma^2 - 8\gamma^4) - 12\gamma^3 y_o + (1 - 8\gamma^2)\, y_o^2 - 2\gamma y_o^3\right] x_o^{-2} \\ & + \left[(-2 + 14\gamma^2 + 35\gamma^4 + 12\gamma^6)\right. \\ & + (35\gamma^3 + 30\gamma^5) y_o + (-2 + 14\gamma^2 + 40\gamma^4) y_o^2 \\ & \left. + 30\gamma^3 y_o^3 + (-1 + 12\gamma^2) y_o^4 + 2\gamma y_o^5\right] x_o^{-4}\} \, e^{-y_o^2}\end{aligned} \tag{46}$$

and

$$\gamma \equiv (m\langle\vec{v}\rangle^2/2kT)^{1/2}, \quad x_o \equiv (E_o/kT)^{1/2},$$

$$y_o \equiv (E_o/kT)^{1/2} - (m\langle\vec{v}\rangle^2/2kT)^{1/2} \tag{47}$$

In Fig. 1, $\Lambda(\gamma,x_o)$ is shown quantitatively in dependence of the energy ratios γ^2 and x_o^2. In general, $\Lambda(\gamma,x_o)$ increases with increasing γ^2 and decreasing x_o^2, except in the region $\gamma^2 \lesssim 10^{-1}$. The formula for dN/dt in Eq. (66) holds only at the surface of the cathode or within a mean free path from the cathode. In comparing this result with experiments, it should be noted that the background gas reduces the number of sputtered atoms observed as its pressure increases.

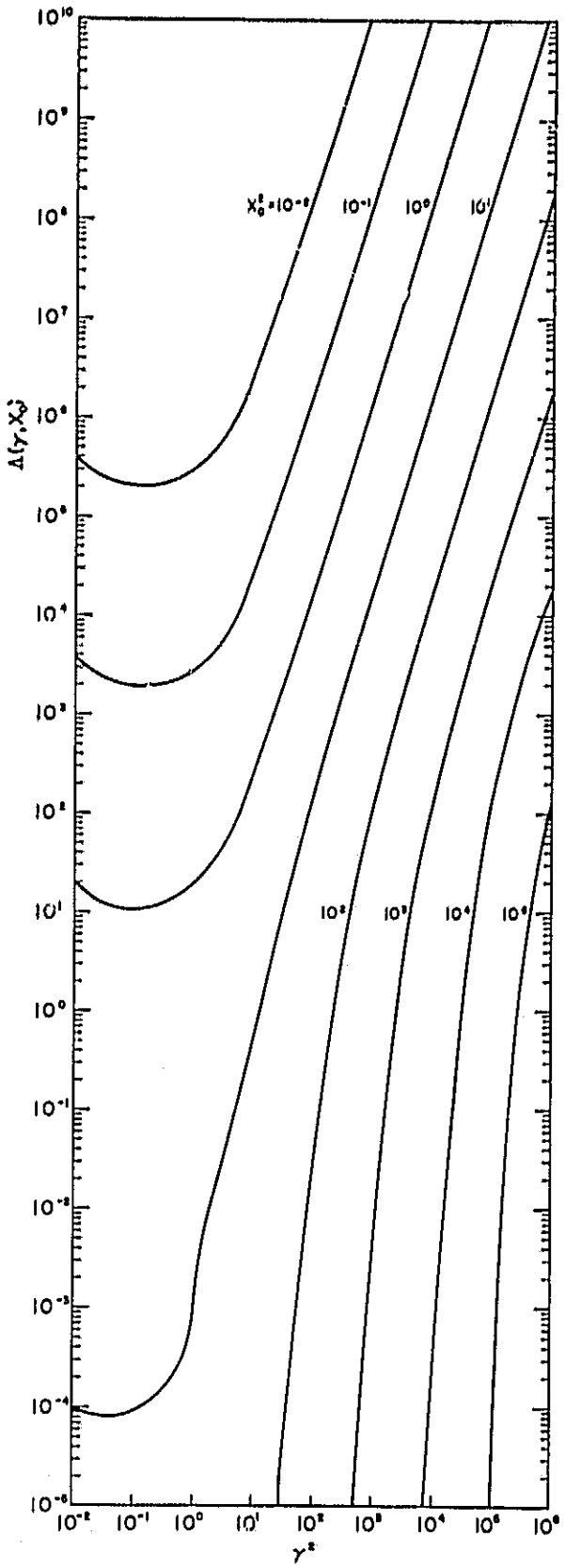

FIG. 1: $\Lambda(\gamma, x_o)$ versus γ^2 with x_o^2 as parameter.

References

1. Sh. G. Askerov and L. A. Sena, Sov. Phys. - Solid State 11, 1288 (1969).

2. R. V. Stuart and G. K. Wehner, J. Appl. Phys. 33, 2345 (1962).

3. F. N. Mott and H. S. Massey, The Theory of Atomic Collisions, At the Clarendon Press, Oxford 1965.

4. H. S. Massey, E. H. Burhop and H. B. Gilbody, Electronic and Ionic Impact Phenomena, At the Clarendon Press, Oxford 1969.

5. L. I. Schiff, Quantum Mechanics, McGraw-Hill, New York 1956.

6. E. Fermi, Nuclear Physics, The University of Chicago Press, Chicago 1963.

7. M. J. Druyvesteyn and F. M. Penning, Rev. Mod. Phys. 12, 87 (1940).

III. TRANSPORT AND DEPOSITION OF SPUTTERING PRODUCTS

As long as the mean free path ℓ of the sputtered particles is very large compared to the distance d between the emitting plane and the surrounding system surfaces, the particles travel undeflected along straight lines determined by their initial velocity at the point of emission. Within this free particle flow, only those system surfaces (a) are reached which can be connected with the emitter plane through straight lines (Fig. 1). Particles interact, however, always more or less weakly independent of how low their concentration is since the interaction forces (polarization forces, electric and magnetic dipole forces, coulomb forces) have infinite range. For this reason, always a few particles will be sufficiently deflected out of their initial path so that they can reach system surfaces (b) which are not "seen" along a straight line by the emitter (Fig. 2). For sputtered particles with a mean free path $\ell >> d$, the deposition on surfaces of type (a) can be calculated in first approximation by free particle flow, whereas the deposition on surfaces of type (b) has to be evaluated by means of a weak interaction diffusion theory. The determination of the diffusion coefficient for the sputtered particles requires the solution of kinetic equations describing the weak but many-particle interactions at on the average large distances. The analysis of deposition by diffusion on system surfaces of the type shown in Fig. 2 leads to a multi-region boundary-value problem with mixed boundary conditions. For these reasons, deposition by diffusion will not be treated.

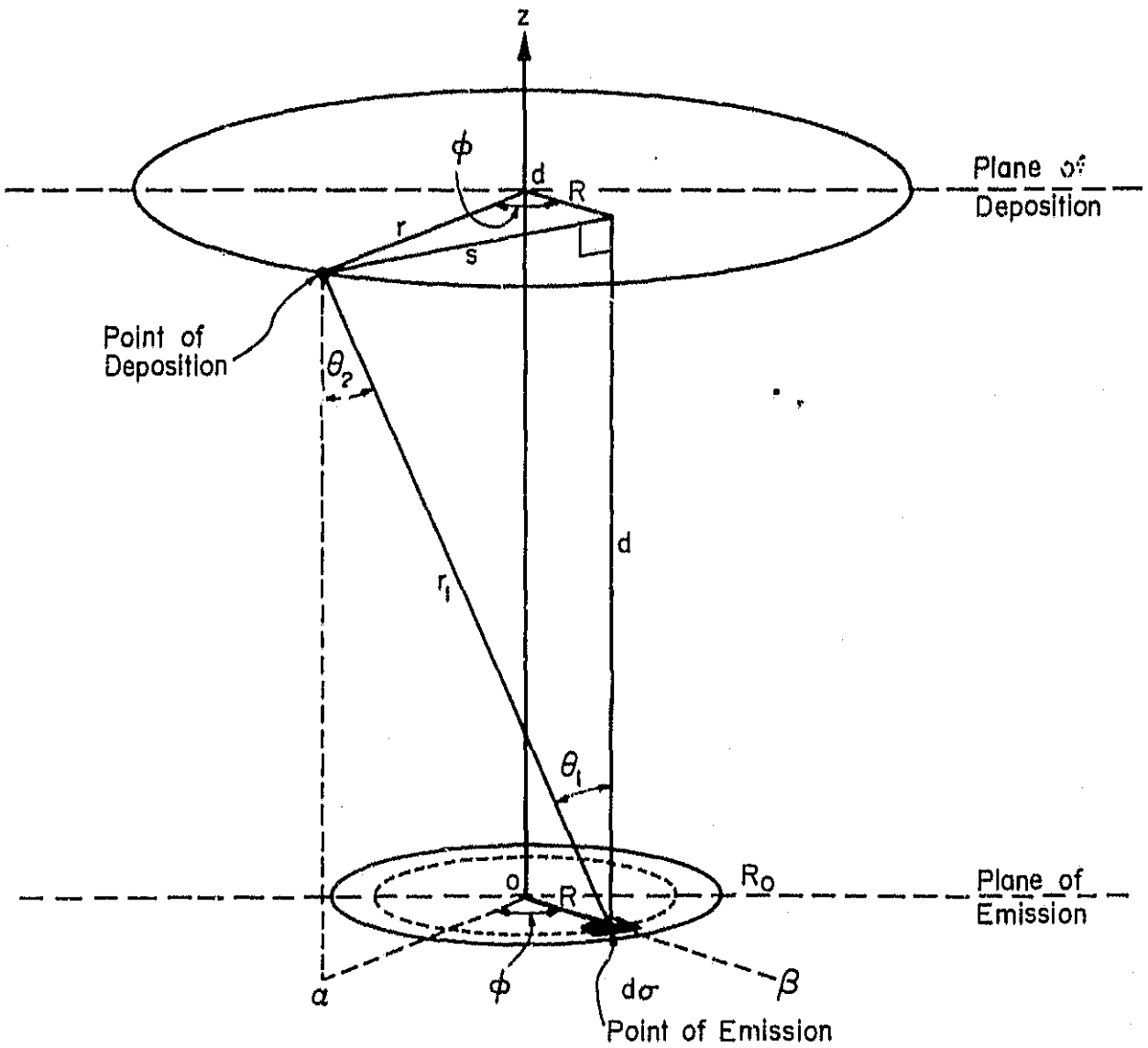

FIG. 1: Geometry of emitter ($z = 0$, $0 \leq R \leq R_o$) and deposition plane ($z = d$, $0 \leq r \leq \infty$).

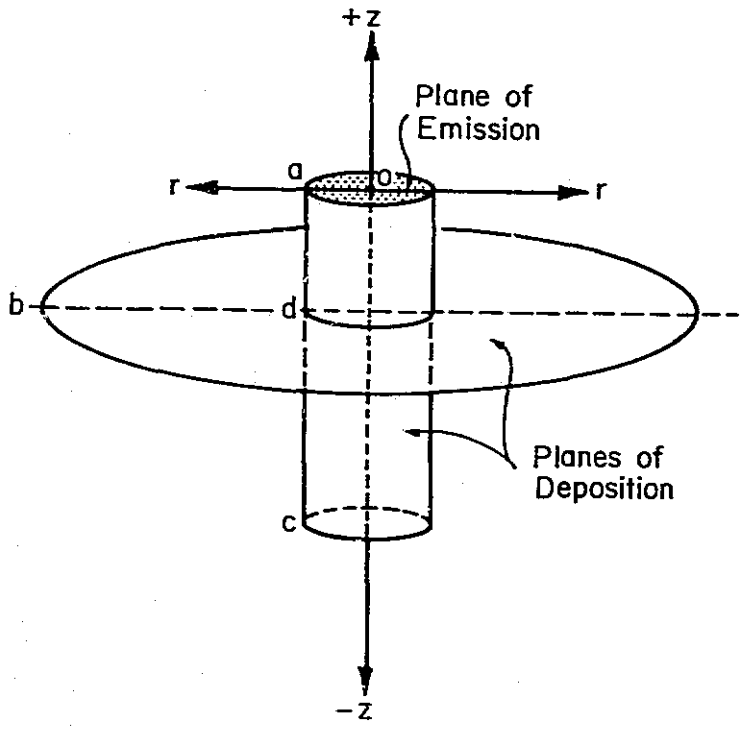

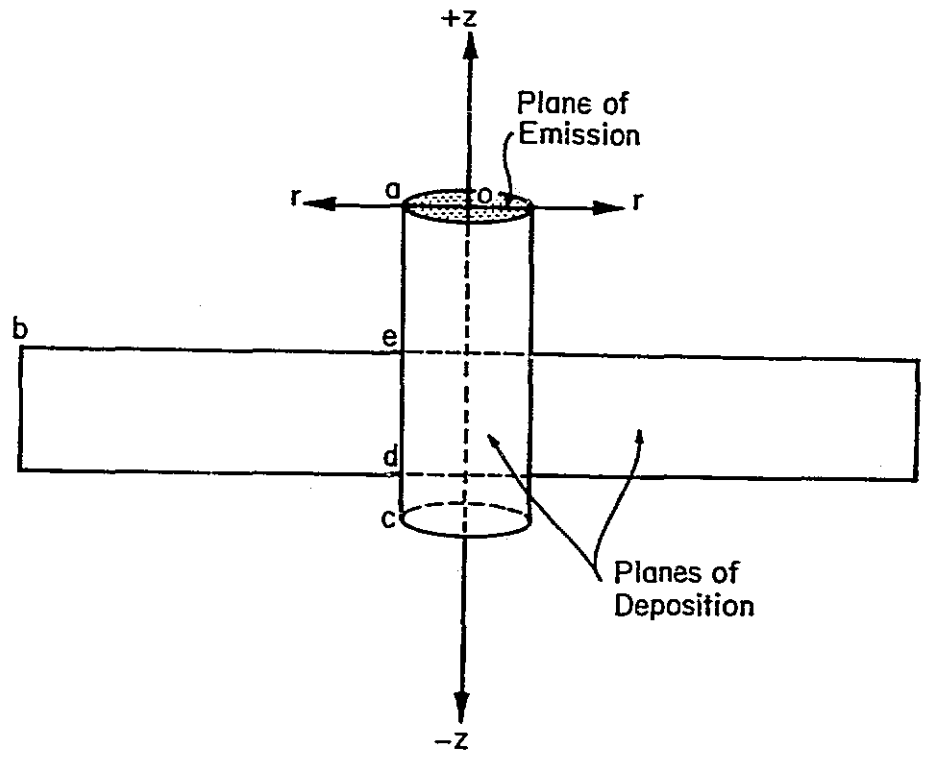

FIG. 2: Examples of deposition planes which can be reached only by particle diffusion.

Within a cylindrical coordinate system (R, β, z), consider an emitting surface of radius $R = R_o$ in the plane $z = 0$. Let the system surfaces, for which the deposition is to be determined, be located in an arbitrary plane $z = d > 0$ (Fig. 1). This general deposition problem is solved by calculating the deposition $j(r, \alpha)$ in an arbitrary point $(r, \alpha, z = d)$ of the infinite "control plane" $z = d$, $0 \leq r \leq \infty$, $0 \leq \alpha \leq 2\pi$. The total deposition on a system surface $r_1 \leq r \leq r_2$, $\alpha_1 \leq \alpha \leq \alpha_2$, $z = d$ is then obtained by integrating $j(r,\alpha)$ over all points (r,α) lying within its boundaries. For ideal free particle flow, the depositions on different finite system surfaces in the plane $z = d$ do not affect each other or the emitting surface. The geometry of Fig. 1 is representative, e.g., for the accelerating grid on an ion thruster from which sputtered atoms are deposited downstream on system surfaces somewhere in the control plane $z = d$.

In the plan $z = 0$, the emitter surface $0 \leq R \leq R_o$, $0 \leq \beta \leq 2\pi$, may emit

$$\Phi = \Phi(R, \beta) \qquad [cm^{-2}\ sec^{-1}] \qquad (1)$$

particles per unit surface and unit time. The rate of deposition at the point (r, α) of the control plane $z = d$ due to a differential source area $d\sigma$ is

$$dj = \Phi(R,\beta)\ \varepsilon(\theta_1, R,\beta)\ \frac{\cos\theta_2}{r_1^2}\ d\sigma \qquad (2)$$

where $\varepsilon(\theta_1, R, \beta)$ is the normalized distribution describing the emission of the particles in the direction θ_1 (Fig. 1) at the point (R,β). It is usually assumed that $\varepsilon(\theta_1, R,\beta)$ is independent of position (R,β) and given by Lambert's cosine law,[1)]

$$\varepsilon(\theta_1,R,\beta) = \cos\theta_1/\pi \quad . \qquad (3)$$

In referring to Fig. 1, it is seen that the following relations hold for geometrical reasons,

$$\theta_1 = \theta_2 \equiv \theta, \qquad \cos\theta = d/r_1 \quad ,$$

$$s^2 = r^2 + R^2 - 2rR\cos\phi \quad ,$$

$$r_1^2 = s^2 + d^2, \qquad \phi = \beta - \alpha \quad ,$$

$$d\sigma = RdR\,d\beta \quad . \qquad (4)$$

Accordingly, the impingement rate $J(r,\alpha)$ in the point (r,α) of the control plane $z = d$ from the entire surface (πR_o^2) of the emitter is

$$J(r,\alpha) = d\int_0^{2\pi}\int_0^{R_o} \frac{\varepsilon(\theta,R,\beta)\Phi(R,\beta)\,RdRd\beta}{[r^2+R^2+d^2-2rR\cos(\beta-\alpha)]^{3/2}} \quad . \qquad (5)$$

The total deposition per unit time on a system surface bounded by the radii r_1 and r_2 and the rays α_1 and α_2 is

$$D(r_{1,2}, \alpha_1) = \int_{\alpha_1}^{\alpha_2}\int_{r_1}^{r_2} J(r,\alpha)\,dr\,d\alpha \quad . \qquad (6)$$

Eq. (5) contains as a special case the deposition equation originally derived by von Hippel.[1)] Equation (5) can be integrated in closed form for cases of practical interest as will be demonstrated next.

1) Uniform Emission Source

In case of a uniform source of sputtered particles which are emitted in accordance with Lambert's law, one has [Eqs. (1) and (3)]:

$$\phi(R,\beta) = \phi_o, \qquad \varepsilon(\theta) = \cos\theta\ /\pi \qquad . \qquad (7)$$

Hence,

$$J(r,\alpha) = \frac{d^2}{\pi}\,\phi_o \int_{-\alpha}^{2\pi-\alpha} \int_0^{R_o} \frac{R\ dR\ d\phi}{[r^2+R^2+d^2 - 2rR\cos\phi]^2} \qquad (8)$$

by Eq. (5) where $\phi = \beta - \alpha$. The ϕ- integral is transformed by means of the substitution $z = \exp(i\phi)$, $d\phi = dz/iz$, $\cos\phi = (z + z^{-1})/2$ as

$$I = \int_{-\alpha}^{2\pi-\alpha} \frac{d\phi}{[p - q\cos\phi]^2} = -i \oint_{|z|=1} \frac{dz}{z[p - \tfrac{1}{2}q(z+z^{-1})]^2}\ ,$$

$$p \equiv r^2+R^2+d^2, \qquad q \equiv 2rR \qquad , \qquad (9)$$

where the point z describes the unit circle as ϕ moves from $-\alpha$ to $2\pi-\alpha$. The integrand in the complex z-plane has poles of second order at each of the points

$$z_{1,2} = -[-p \pm (p^2-q^2)^{\frac{1}{2}}]/q \qquad . \qquad (10)$$

Since $p > q > 0$, the pole z_2 lies outside the unit circle. The residue of the pole z_1 is

$$R = \lim_{z\to z_1} \left\{ \frac{4}{q^2} \frac{d}{dz} \left[\frac{z(z-z_1)^2}{(z-z_1)^2(z-z_2)^2} \right] \right\} = -\frac{4}{q^2} \frac{z_1+z_2}{(z_1-z_2)^3} \ . \qquad (11)$$

After replacing z_1 and z_2 in accordance with Eq. (10), Cauchy's integral theorem yields

$$I = -i\,2\pi i R = 2\pi p/(p^2-q^2)^{3/2} \qquad (12)$$

Hence,

$$J(r,\alpha) = d^2\Phi_o \int_0^{Ro} \frac{(r^2+R^2+d^2)\,dR^2}{[(r^2+R^2+d^2)^2-4r^2R^2]^{3/2}} \qquad (13)$$

This is an integral of standard type[2] which is readily evaluated. The resulting impingement rate is

$$J(r,\alpha) = \tfrac{1}{2}\Phi_o\left\{1 + \frac{R_o^2 - d^2 - r^2}{[(R_o^2 + d^2 - r^2)^2 + 4r^2d^2]^{1/2}}\right\}. \qquad (14)$$

The impingement rate at the point (r,α) of the control plane $z = d$ is independent of the azimuthal position α since ε and Φ are independent of β [Eqs. (7) and (9)].

2) Parabolic Emission Source.

For a parabolic source of sputtered particles which are emitted in accordance with Lambert's law, the Eqs. (1) and (3) become

$$\Phi(R,\beta) = \Phi_o\left(1 - \frac{R^2}{R_o^2}\right), \quad \varepsilon(\theta) = \cos\theta/\pi \qquad (15)$$

Hence

$$J(r,\alpha) = \frac{d^2}{\pi}\,\Phi_o \int_{-\alpha}^{2\pi-\alpha} \frac{[1-(R^2/R_o^2)]\;R\,dR\,d\phi}{[r^2+R^2+d^2 - 2rR\cos\phi]^2} \qquad (16)$$

by Eq. (5) where $\phi = \beta - \alpha$. Upon substitution of the ϕ-integral evaluated in Eq. (12), Eq. (16) is reduced to

$$J(r,\alpha) = \tfrac{1}{2}\,\Phi_o\left\{1 + \frac{R_o^2 - d^2 - r^2}{[(R_o^2 + d^2 - r^2)^2 + 4r^2d^2]^{1/2}}\right\}$$

$$- \frac{d^2}{R_o^2}\,\Phi_o \int_0^{R_o} \frac{(R^2 + d^2 + r^2)\,R^2\,dR^2}{[(R^2 + d^2 - r^2)^2 + 4r^2d^2]^{3/2}}. \qquad (17)$$

The latter integral is evaluated by standard methods[2]. The resulting impingement rate at the point (r,α) of the control plane $z = d$ is

$$J(r,\alpha) = \tfrac{1}{2}\Phi_o \left\{ 1 + \frac{R_o^4 + 2R_o^2(d^2 - r^2) + (d^2 + r^2)^2}{R_o^2 [R_o^2 + d^2 - r^2)^2 + 4r^2d^2]^{\frac{1}{2}}} - \frac{d^2}{R_o^2}\left[1 + \frac{r^2}{d^2} + 2\,\ln\left(\frac{R_o^2 + d^2 - r^2 + [(R_o^2 + d^2 - r^2)^2 + 4r^2d^2]^{\frac{1}{2}}}{2d^2} \right)\right] \right\} \tag{18}$$

$J(r,\alpha)$ is the same for any azimuth $0 \leq \alpha \leq 2\pi$ since ε and Φ are independent of β. The parabolic source distribution [Eq. (15)] is a first approximation to the nonuniform emission of atoms from the accelerating grid of an ion thruster (presumed that the density of the sputtering charge exchange ions decreases parabolically with increasing R).

3) Arbitrary Nonuniform Emission Source.

In many experimental situations, the source $\Phi = \Phi(R,\beta)$ is a complicated function of both R and β with symmetry and boundary properties of the form

$$\Phi(R_o,\beta) = 0, \qquad \Phi(R,-\beta) = \Phi(R,+\beta) \quad ,$$

$$d\Phi(0,\beta)/dR = 0 \quad . \tag{19}$$

The emission coefficient is again assumed to be given by Lambert's law,

$$\varepsilon(\theta) = \cos\theta/\pi \quad . \tag{20}$$

In this case, it is mathematically suitable to expand $\Phi(R,\beta)$ in a

Fourier series,

$$\Phi = \Phi_o + \sum_{m=0}^{\infty}{}' \sum_{n=0}^{\infty} \Phi_{mn} \cos m\beta \cos \frac{2n+1}{2}\pi \frac{R}{R_o} \qquad (21)$$

where

$$\Phi_{mn} = \frac{2}{\pi R_o} \int_0^{2\pi} \int_0^{R_o} \Phi(R,\beta)\cos m\beta \cos \frac{2n+1}{2}\pi \frac{R}{R_o}\, dR\, d\beta,$$

$$\Phi_o = \frac{1}{2\pi R_o} \int_0^{2\pi} \int_0^{R_o} \Phi(R,\beta)\, dR\, d\beta \quad . \qquad (22)$$

Eq. (21) is a complete expansion for an arbitrary function $\Phi(R,\beta)$ subject to the conditions in Eq. (19). Insertion of Eqs. (20) - (21) into Eq. (15) yields, under consideration of Eq. (14),

$$J(r,\alpha) = \frac{1}{2}\Phi_o \left\{ 1 + \frac{R_o^2 - d^2 - r^2}{[(R_o^2+d^2-r^2)^2 + 4r^2d^2]^{1/2}} \right\} + \tilde{J}(r,\alpha) \qquad (23)$$

where

$$\tilde{J}(r,\alpha) = \frac{d^2}{\pi} \sum_{m=0}^{\infty}{}' \sum_{n=0}^{\infty} \Phi_{mn} \int_{-\alpha}^{2\pi-\alpha} \int_0^{R_o} \frac{\cos m(\phi+\alpha) \cos \frac{2n+1}{2} \frac{R}{R_o}\, R\, dR\, d\phi}{[r^2+R^2+d^2-2rR\cos\phi]^2}. \qquad (24)$$

By means of substitutions similar to those under a), $z = \exp(i\phi)$,..., $\cos m(\phi + \alpha) = Re[z^m \exp(im\alpha)]$, the ϕ-integral in Eq. (24) is transformed as

$$I_m = \int_{-\alpha}^{2\pi-\alpha} \frac{\cos m(\phi+\alpha)\, d\phi}{[p-q\cos\phi]^2}$$

$$= \frac{4}{q^2} Re \left\{ \frac{e^{im\alpha}}{i} \oint_{|z|=1} \frac{z^{m+1}\, dz}{[z^2 + 2pq^{-1} z + 1]^2} \right\} \quad . \qquad (25)$$

where the integration path is the unit circle in the complex z-plane.

The integrand has poles of the second order at each of the points

$$z_{1,2} = -[-p \pm (p^2-q^2)^{1/2}]/q \quad . \qquad (26)$$

Since $p > q > 0$, z_2 lies outside of the unit circle, the residue at the point z_1 is

$$R = \lim_{z\to z_1} \frac{d}{dz}\left[\frac{z^{m+1}(z-z_1)^2}{(z-z_1)^2(z-z_2)^2}\right]$$

$$= z_1^m\left[-\frac{z_1+z_2}{(z_1-z_2)^3} + \frac{m}{(z_1-z_2)^2}\right]$$

$$= \frac{q^2}{4}\left[\frac{p-(p^2-q^2)^{1/2}}{q}\right]^m \left[\frac{p}{(p^2-q^2)^{3/2}} + \frac{m}{p^2-q^2}\right] \qquad (27)$$

by Eq. (26). According to Eqs. (25) and (27) and the residue theorem

$$I_m = 2\pi \cos m\alpha\left[\frac{p-(p^2-q^2)^{1/2}}{q}\right]^m \left[\frac{p}{(p^2-q^2)^{3/2}} + \frac{m}{p^2-q^2}\right]. \qquad (28)$$

Thus, one finds, upon substitution of Eq. (28) into Eq. (24), that

$$\tilde{J}(r,\alpha) = 2d^2 \sum_{m=0}^{\infty}\sum_{n=0}^{\infty} \Phi_{mn} \cos m\alpha \int_0^{R_o}\left\{\frac{p(R)-[p^2(R)-q^2(R)]^{1/2}}{q(R)}\right\}^m *$$

$$* \left\{\frac{p(R)}{[p^2(R)-q^2(R)]^{3/2}} + \frac{m}{p^2(R)-q^2(R)}\right\} \cos\frac{2n+1}{2}\pi\frac{R}{R_o}\, RdR, \qquad (29)$$

where

$$p(R) \equiv p(R,r,d) = r^2+d^2+R^2, \quad q(R) \equiv q(R,rd) = 2rR \quad . \qquad (30)$$

The impingement rate $\tilde{J}(r,\alpha)$ depends both on r and α since $\Phi(R,\beta)$ varies with azimuthal position β. It is seen that the m-th

Fourier component in Eq. (29) contributes an α- dependence in the simple form cos $m\alpha$. A two-dimensional emission $\phi(R,\beta)$ satisfying the conditions in Eq. (19) is, e.g., observed at the accelerating grid of ion thrusters if the grid holes are arranged at equal azimuthal spacings $\Delta\phi(r)$ along concentric circles $r = \text{const} < R_o$. The remaining R-integrals in Eq. (29), in particular those with large m, are most conveniently evaluated numerically.

References

1. A. von Hippel, Ann. d. Physik 80, 672 (1926); 81, 1043 (1926).

2. W. Groebner and H. Hofreiter, Integral Tables, I, Springer-Verlag, Vienna 1960.

IV. KINETIC THEORY OF LOW PRESSURE GAS DISCHARGE

The theoretical evaluation of electrical discharges by means of macroscopic or kinetic equations is one of the classical, unsolved problems of plasma physics. To date, no progress has been made in calculating the potential distribution in electrical discharges from first principles. Although a rigorous theory of the electron diode with explicit boundary conditions in vacuum based on the Vlasov equation is known,[1] a treatment of the corresponding electron-ion diode in vacuum (no ionization) is missing in the literature. In the following, a kinetic theory for a low pressure discharge will be formulated. The mathematical difficulties resulting from the production of the ions by volume ionization (electron-neutral collisions) and the complex functional boundary conditions for the electron and ion velocity distributions are discussed within the frame of the Vlasov theory.[1]

In an electrical discharge, the current carriers are generated both within the volume of the plasma and at the electrodes. As the pressure decreases, the electrons are produced mainly at the cathode by secondary processes and thermal emission, whereas the main source for ions is still volume ionization since emission and production of ions at the electrodes is negligible. For this type of low pressure discharge, the velocity distributions of the electrons and ions are determined by Vlasov equations which are coupled by the Poisson equations for the self-consistent electric field and th sources due to volume ionization. The corresponding nonlinear boundary-value problem has functional boundary conditions which result from the various electrode processes.

In order to reduce the mathematical formalism, a one-dimensional discharge geometry with parallel plate electrodes of infinite extension is assumed.

Consider a low pressure discharge plasma [Debye radius $D = (\sum 4\pi r_s e_s^2/kT_s)^{-1/2} \ll a$] between a plane cathode (x=0) and a plane anode (x=a). The mean free paths of the electrons, ions, and neutral atoms are assumed to be large compared to the electrode distance, $\ell_s \gg a$ (so-called "collision-free" plasma). In the one-dimensional case, the velocity distribution functions of the electrons, $f = f(v,x)$, and the ions, $F = F(V,x)$, in the self-consistent field $E = -d\phi(x)/dx$ are described by the Vlasov equations[1)]

$$v \frac{\partial f}{\partial x} + \frac{e}{m} \frac{d\phi}{dx} \frac{\partial f}{\partial v} = \lambda \sigma(v,x) \quad , \qquad (1)$$

$$V \frac{\partial F}{\partial x} - \frac{e}{M} \frac{d\phi}{dx} \frac{\partial F}{\partial V} = \lambda \Sigma(V,x) \quad , \qquad (2)$$

where

$$\frac{d^2\phi}{dx^2} = 4\pi e \int_{-\infty}^{+\infty} f(v,x)\, dv - 4\pi e \int_{-\infty}^{+\infty} F(V,x) dV \qquad (3)$$

is the field-source equation. The electron and ion sources due to volume ionization can be reduced to the expressions,

$$\sigma(v,x) = \nu f(v,x)\, H[v - (2I/m)^{1/2}] \quad , \qquad (4)$$

$$\Sigma(V,x) = \nu g_o(V) \int_{-\infty}^{+\infty} f(v,x)\, dv \quad , \qquad (5)$$

where,

$$\nu = N_o \langle \sigma(v)\, v \rangle \quad , \qquad (6)$$

$$g_o(V) = (M/2\pi kT_o)^{3/2}\ e^{-\frac{1}{2}MV^2/kT} \quad , \qquad (7)$$

and

$$H(v - v_o) = 1, \qquad v \geq v_o > 0 \quad ,$$

$$= 0, \qquad v \leq v_o > 0 \quad , \qquad (8)$$

is the Heavyside step function. In Eqs. (1) - (6), $e = -e$, and $e_i = +e$, are the charges, m and M are the masses, and v and V are the individual velocities of the electrons and ions, respectively. N_o and T_o are the density and temperature of the neutrals, and $\sigma(v)$ is their ionization cross section in dependence of the electron velocity which is assumed to be large compared to the heavy particle velocity, $|v| >> |V|$. I is the ionization energy.

Within the self-consistent field model for long range Coulomb interactions, usually (elastic and inelastic) short-range binary interactions are not regarded [$\lambda \to 0$ in Eqs. (1) - (2)]. The Boltzmann collision integral destroys the "simple" integral-functional structure of the original Vlasov equation. For this reason, the Boltzmann collsion integral for ionization has been approximated in Eq. (1) by the discontinuous relaxation expression in Eq. (4). The associated ion source in Eq. (2) is then given by Eq. (5) with $g_o(V)$ being the Maxwellian in Eq. (7). (The latter presumes that the neutral atoms are in thermal equilibrium.) It should be noted that volume ionization must be included in the physical model for the discharge since otherwise only a trivial solution $F = 0$ of Eq. (2) would exist. On the other hand, the elastic binary interactions of the electrons or

ions with the neutrals can be neglected compared to the self-consistent long range interactions.

The boundary conditions for the potential $\Phi(x)$ are given by the fixed potentials at the cathode (Φ_o) and anode (Φ_a). In contrast to Φ_o and Φ_a, the boundary conditions for the distributions $f(v,x)$ and $F(V,x)$ are not known explicitly. The latter boundary conditions are given implicitly by the surface processes at the cathode and anode of the low pressure discharge, i.e.:

i) Reflection of electrons at the cathode (x=0) and anode (x=a) [reflection coefficient: $R^e_x = R^e_x(\frac{1}{2} mv^2)$].

j) Thermal emission of electrons at the cathode [thermal emission distribution: $f_T = f_T(\frac{1}{2} mv^2)$].

k) Secondary emission of electrons at the cathode by incident ions [probability of emission of an electron of energy $\frac{1}{2} mv^2$ by an ion of energy $\frac{1}{2} MV^2$: $S = S(\frac{1}{2} mv^2 | \frac{1}{2}MV^2)$].

ℓ) Neutralization and absorption of the ions at the electrodes [effective reflection coefficient: $R^i_x = R^i_x(\frac{1}{2} MV^2)$].

Accordingly, the boundary conditions for the fields $f(v,x)$, $F(V,x)$, and $\Phi(x)$ are:

$$f(x=0,\ v > 0) = f_T(\tfrac{1}{2} mv^2) + R^e_o(\tfrac{1}{2} mv^2)\ f(x=0,\ v < 0) + S(\tfrac{1}{2} mv^2 | \tfrac{1}{2} MV^2)\ \ F(x=0,\ V < 0) \quad , \qquad (9)$$

$$f(x=a,\ v < 0) = R^e_a(\tfrac{1}{2} mv^2)\ f(x=a,\ v > 0) \quad , \qquad (10)$$

$$F(x=0,\ V > 0) = R^i_o(\tfrac{1}{2} MV^2)\ F(x=0,\ V < 0) \cong 0 \quad , \qquad (11)$$

$$F(x=a,\ V < 0) = R^i_a(\tfrac{1}{2} MV^2)\ F(x=a,\ V > 0) \cong 0 \quad , \qquad (12)$$

and

$$\Phi(x=0) = \Phi_o, \qquad \Phi(x=a) = \Phi_a \quad . \qquad (13)$$

Thus, one finds that a low pressure discharge is described by a boundary-value problem for nonlinear integro-differential equations [Eqs. (1) - (3)] with regular [Eq. (13)] and functional [Eqs. (9) - (12)] boundary conditions. For statistical equilibrium and negligible field emission, f_T is given by[2)]

$$f_T = \frac{m^2 kT}{2\pi\hbar^2} e^{-(\frac{1}{2} mv^2 + \varepsilon_m - \zeta)/kT} [1 - R_o^e(\tfrac{1}{2} mv^2)] \, H(v) \qquad (14)$$

where T is the cathode temperature, ε_m is the barier energy of the metal and $\zeta \cong \zeta_o$ is the Fermi energy. Neglecting quantum mechanical tunneling, the reflection coefficient of the electrodes is[3)]

$$R^e = [(1 + \frac{\frac{1}{2} mv^2}{\varepsilon_m})^{1/2} - (\frac{\frac{1}{2} mv^2}{\varepsilon_m})^{1/2}]^4 \quad . \qquad (15)$$

On the other hand, nearly all the ions are neutralized as they approach a metal surface so that their effective reflection coefficient is

$$R^i \cong 0 \quad . \qquad (16)$$

The secondary electron emission probability $S(\frac{1}{2} mv^2 | \frac{1}{2} MV^2)$ has to be determined from experimental data since no convincing theory is available. The Eqs. (14) - (16) give essentially the correct magnitude of the surface effects. A more sophisticated description is not attempted since this would render the boundary conditions too complicated. The Eqs. (1) - (16) represent probably the most simple theoretical formulation of the physical problem under consideration.

In spite of the physical simplifications, the above nonlinear boundary-value problem turns out to be extremely difficult. This is mainly due to the source terms $\sigma(v,x)$ and $\Sigma(V,x)$ in Eqs. (1) - (2). If one treats volume ionization as a small perturbation, then Eqs. (1) - (2) reduce to the ideal Vlasov equations in first approximation ($\lambda \to 0$):

$$v \frac{\partial f}{\partial x} + \frac{e}{m} \frac{d\Phi}{dx} \frac{\partial f}{\partial v} = 0 , \qquad V \frac{\partial F}{\partial x} - \frac{e}{M} \frac{d\Phi}{dx} \frac{\partial F}{\partial V} = 0 \quad , \qquad (17)$$

which have generalized functional similarity solutions of the form

$$f = P[\tfrac{1}{2} mv^2 - e\Phi(x)], \qquad F = Q[\tfrac{1}{2} MV^2 + e\Phi(x)] . \qquad (18)$$

P and Q are arbitrary discontinuous functions [because of the hyperbolic nature of Eq. (17)] of the functional argument indicated which have to be determined in such a way that the boundary conditions in Eqs. (9) - (12) are satisfied. This perturbation approach does, however, not work in absence of volume ionization ($\lambda=0$) since $F(v,x) = Q \equiv 0$ because of the homogeneity of the boundary conditions for $F(v,x)$ [Eq. (12)]. For this reason, a more general functional similarity solution has to be derived for the complete Eqs. (1) - (2) with volume ionization ($\lambda=1$). This could not be accomplished, however, in spite of a considerable effort in time. It is hoped that the solution of this gas discharge problem can be reported at a later date.

References

1. A. A. Vlasov, Many-Particle Theory and its Application to Plasma, Gordon and Breach, New York 1961.

2. S. Dushmann, Rev. Mod. Phys. 2, 382 (1930).

3. L. Nordheim, Z. Phys. 46, 833 (1928).

4. H. D. Hagstrum, Phys. Rev. 123, 758 (1961).